

## Activated carbons from bituminous coals; a comparison of H<sub>3</sub>PO<sub>4</sub> and KOH activants

Marit Jagtoyen, Chris Toles and Frank Derbyshire

University of Kentucky Center for Applied Energy Research  
3572 Iron Works Pike, Lexington, KY 40511-8433

### INTRODUCTION

An earlier study was made of the generation of activated carbons from bituminous coals, using phosphoric acid as a chemical reagent [1-4]. Other work has shown that potassium hydroxide is an effective reagent for the production of high surface area carbons from starting materials such as brown coal [5,6], and other coals, petroleum coke, or mixtures of these [7]. High surface area carbon fibres can also be prepared from charcoal cloth (carbonized viscose rayon cloth) by chemical activation with alkali hydroxides such as KOH at 500°C [8].

For these reasons, the research has been extended to examine the relative effectiveness of H<sub>3</sub>PO<sub>4</sub> and KOH as activants for the synthesis of activated carbons from bituminous coal, and the influence of these reagents on reaction mechanisms, porosity development, and adsorptive properties.

### EXPERIMENTAL

An Illinois Basin bituminous coal (IBC 106) was supplied by the Illinois Basin Coal Sample Program. Before being used for carbon synthesis, the coal was first ground and cleaned to lower the ash content, using a laboratory scale flotation unit [2]. Properties of the parent and cleaned coals are given in Table 1.

The carbon synthesis procedure has been described in detail elsewhere [2,4]. Briefly, a 20 g sample of dry coal is thoroughly mixed with a given volume of reagent solution at room temperature. The mixture is then reacted first at a low heat treatment temperature (HTT), and subsequently at a higher HTT, in both cases in flowing nitrogen. The solid products are leached with distilled water to pH=6 and vacuum dried at 110°C before further analysis. The tar and oil products are collected in cold traps, and gaseous products are collected in a calibrated graduated gas cylinder.

The conditions normally used with H<sub>3</sub>PO<sub>4</sub> were: wt. ratio of acid to dry coal= 0.96, added as 30 cm<sup>3</sup> of 50% acid solution; low HTT 170°C for 0.5 to 3h; upper HTT 350 - 650°C for 1h. The corresponding conditions for KOH were: weight ratio=1.42 of KOH to dry coal, added as 28.4 g KOH to 20 g coal in 100 cm<sup>3</sup> H<sub>2</sub>O; low HTT 75°C for 2h; upper HTT 400 - 900°C for 1h. In some experiments, the reagent to coal ratio was varied. Thermal blank experiments were performed under the same conditions for comparison.

The leached and dried heat treated solids were routinely analyzed for H, C, O, N, S, ash and moisture contents. Fourier transform infrared (FTIR) spectra were obtained from 0.4% loaded KBr discs using a Nicolet 20SX spectrophotometer.

Surface area measurements were obtained from nitrogen adsorption isotherms at 77 K using a Quantachrome Autosorb 6 apparatus. Specific surface areas, S<sub>BET</sub>, were obtained from the adsorption isotherms using the BET equation. Mesopore surface areas were obtained using the α<sub>s</sub> method [9]; standard isotherm data were taken from Rodriguez-Reinoso et al. [10].

## RESULTS AND DISCUSSION

### *Chemical Change*

Both reagents promote chemical change at lower temperatures and more extensively than is achieved by thermal reaction. The H/C atomic ratio of carbons produced by different treatments is shown as a function of HTT in Figure 1. In the presence of either activant, dehydrogenation is considerably enhanced [2,4]. Gas analyses have shown that significant quantities of hydrogen may be evolved during chemical activation: for KOH activation up to 70-90% of the parent coal hydrogen is released as H<sub>2</sub>, around 7% with H<sub>3</sub>PO<sub>4</sub> treatment, and a negligible amount on thermal treatment. In parallel with these observations, Fourier transform infrared spectroscopy of the carbons shows that chemical activation results in the earlier disappearance of aliphatic absorption bands.

The oxygen content of the carbon products was determined by difference, and hence there is a reasonable margin of error in the data. With this caveat, it seems that the oxygen content of H<sub>3</sub>PO<sub>4</sub> carbons falls quickly with HTT, from 12% in the starting coal to about 5% by 350°C, and remains in the range 3-5% between 350 and 650°C. The pattern is different for KOH, where there appears to be an initial reduction in oxygen content, followed by an increase at 400-500°C to values higher than that in the parent coal. Subsequently, the oxygen content is reduced, falling to negligible values at 800 and 900°C. With both reagents, FTIR spectroscopy shows the appearance of carbonyl absorption bands at temperatures from about 75 to 500°C. This band is not evident in the thermal products, and the formation of C=O groups appears to be an intrinsic part of the chemical activation mechanism. Presumably, at high HTT, the carbonyl groups are eliminated by thermal reaction: CO and CO<sub>2</sub> begin to be evolved at HTT over same temperature range where the C=O adsorption bands are reduced in intensity.

Reaction with H<sub>3</sub>PO<sub>4</sub> or KOH effects the removal of both inorganic and organic sulfur. Pyritic sulfur is eliminated with relative ease, while some residual organic sulfur remains to high HTT, Figure 2. The mode of sulfur removal is found to depend upon the reagent used: with phosphoric acid, a large proportion of sulfur is liberated as H<sub>2</sub>S [1,2,4], whereas with KOH it is released as a water-soluble sulfide during leaching of the heat treated solid, Figure 3. Some sulfatic sulfur is also produced upon KOH activation. Research with model compounds has shown that dibenzothiophene, benzothiophene and thiophenol are desulfurized by reaction with bases, such as KOH, at 375 - 400°C. Ring opening is followed by sulfur removal, probably as a soluble potassium sulfide. Oxygen-containing analogs, indole and benzofuran, also experience ring-opening but no subsequent loss of the heteroatom [11]. Analogous behavior can be anticipated for H<sub>3</sub>PO<sub>4</sub>, with the sulfur released as H<sub>2</sub>S instead of K<sub>2</sub>S.

### *Porosity*

The ratio of reagent to precursor is important to the development of carbon pore structure. As shown in Figure 4, a minimum weight ratio is required to maximize the BET surface area: approximately 0.75 to 1.0 for H<sub>3</sub>PO<sub>4</sub> and 1.0 to 1.3 for KOH. At higher ratios, the specific BET surface area decreases. In both series of carbons, there were significant increases in ash content at the highest ratios (9.1% for H<sub>3</sub>PO<sub>4</sub> and 11.2% for KOH). It can be concluded that there is no gain to be made from using excess reagent, since it is consumed by reaction with coal mineral matter to form insoluble products [3], and it lowers the surface area per unit mass. If it is assumed that the ash has negligible porosity, then expressing the surface area on an ash-free basis should compensate for this reduction. As shown in the figure, this appears to be the case.

Operating above the minimum ratios, the development of BET surface area is shown as a function of HTT in Figure 5. The two series of chemically activated carbons develop similar surface areas up to HTT of about 500°C. At higher temperatures, the microporosity of the phosphoric acid carbons decreases slightly from a maximum surface area around 840 m<sup>2</sup>/g, while that of the KOH-activated carbons continues to increase: at HTT 900°C, the BET surface area approaches 1700 m<sup>2</sup>/g. Evidently, the two reagents have quite different temperature dependencies. The thermal products

have negligible accessible surface area, and would have to be subjected to partial gasification in steam or  $\text{CO}_2$  to open up the pore structure.

The ash content of the  $\text{H}_3\text{PO}_4$  carbons increases with temperature from 3.0% at 350°C to 12.0% at 650°C. In contrast to the behavior found with increasing the ratio KOH: coal, the ash content of the KOH carbons decreases with HTT from 6.9% at 400°C to 3.7% at 900°C: a similar observation has been made in related studies [12]. Expressing the data on an ash-free basis, shows that the maximum in the surface area of the  $\text{H}_3\text{PO}_4$  carbons is flattened, Figure 5. However, the correction does not eliminate the possibility of its existence. Other studies with subbituminous coal, coconut shell and wood precursors [13, 14, 15] have also shown the existence of maxima in surface area at similar HTT. The low ash content of the biomass precursors, and the sharpness of the reported maxima render it unlikely that increases in ash content of the carbons can account for the loss of surface area at high HTT. The more likely causes are considered to be due to the acid becoming inactive for the promotion of further porosity development, and the influence of dimensional contraction of the carbon at high HTT [15].

The mesopore capacities of the chemically activated carbons are low and in the range 20 - 75  $\text{m}^2/\text{g}$ . For the KOH carbons, there is no clear trend with increasing HTT, whereas that of the  $\text{H}_3\text{PO}_4$  carbons passes through a shallow maximum at 500-550°C.

It is supposed that, at lower HTT, the chemical reagents promote the formation of crosslinks within the coal structure by ionic mechanisms, leading to the establishment of a rigid, three-dimensional matrix, that is less prone to volatile loss and volume contraction upon heating to higher temperatures. The formation of a crosslinked structure can help to preserve the elements of porosity in the starting material. These suppositions, and the implicit assumption of increased carbon yield have been demonstrated by other work on the phosphoric acid activation of white oak [15]. This more recent work on the activation of white oak has shown that acid treatment actually causes an expansion of the structure that corresponds directly to porosity development. In comparison, extensive shrinkage of the thermal products leads to a collapse of the pore system, making it more difficult to access until carbon is removed by partial gasification.

At high HTT, there is a continuing development of surface area upon KOH activation, and an increase in amount of CO released to the gas phase. On the other hand, with  $\text{H}_3\text{PO}_4$  treatment, there is clearly no further increase in surface area above about 500°C. It is known that, with increasing temperature, orthophosphoric acid undergoes progressive dehydrogenation [16]. Above about 400°C, extensive polymerization and the elimination of water leads to the formation of metaphosphoric acid ( $\text{HPO}_3$ )<sub>n</sub>. The formation of polyphosphates is also indicated by measurements by  $^{31}\text{P}$  NMR and FTIR. This species may be inactive with respect to porosity development, and further increase in HTT above 500°C results in volume contraction accompanied by a reduction in surface area. The same phenomenon could be explained by a structural rearrangement and associated contraction, if the crosslinks formed at low HTT have reached their limit of thermal stability.

### *Adsorptive properties*

The synthesized carbons were subjected to standard test methods to assess their utility [17, 18]. The iodine number provides an indication of the adsorption capacity for small molecules and is usually found to be directly proportional to the BET surface area. The determination was made for a suite of KOH activated carbons, and not surprisingly the highly microporous KOH carbons gave high values for the iodine number.

The methylene blue molecule is much larger than iodine, and its adsorption is restricted mainly to the mesopores. It is a useful indicator of the ability of the carbons to adsorb larger molecules, such as colour bodies from solution. A positive relationship was found between mesopore volume and the methylene blue value for a number of phosphoric acid activated carbons. However, the methylene blue values were low, consistent with the low mesopore surface areas; the values for KOH activated carbons were still lower. It may be concluded that these carbons are not ideally suited for the adsorption of large molecules.

Phenol adsorption capacity can be used to assess a carbon's performance for adsorbing polar compounds. Many of the KOH activated carbons proved to be able to adsorb phenol to a similar extent as a commercial water treatment carbon. The capacity of the acid activated carbons was much less, and disproportionately lower than could be explained by the differences in surface area. Phenol, being a polar molecule, will be attracted to polar sites in the carbon, and it is possible that KOH activation produces carbons with more favorable surface chemistry.

## SUMMARY

In the synthesis of activated carbons from bituminous coal using  $H_3PO_4$  and KOH, it is found that both reagents promote chemical change: the removal of hydrogen, oxygen, and organic and inorganic sulfur. Upon KOH activation, up to 70-90% of the parent coal hydrogen can be released as  $H_2$ , and much less upon reaction with  $H_3PO_4$ . Both inorganic and organic sulfur are eliminated; pyritic sulfur removal is relatively facile but some residual organic sulfur remains to high HTT. The mechanism for sulfur removal depends upon the reagent: with phosphoric acid, a large proportion of sulfur is liberated as  $H_2S$  and with KOH much is released as a water-soluble sulfide.

The extent of porosity development is found to be influenced by the ratio of reagent to precursor: a minimum ratio is required to maximize the BET surface area. With increasing HTT, the chemically activated carbons develop similar surface areas up to about 500°C. At higher temperatures, the microporosity of the phosphoric acid carbons decreases slightly, while that of the KOH-activated carbons continues to increase. The mesopore capacities of both series of chemically activated carbons are low and in the range 20 - 75  $m^2/g$ . The thermal products have negligible accessible surface area.

The mechanism of chemical activation is considered to involve the formation of crosslinks at low HTT, leading to the establishment of a rigid, three-dimensional matrix, that is less prone to volatile loss and volume contraction upon heating to higher temperatures. The resulting structure can help to preserve the elements of porosity in the starting material. With KOH, there is continuing development of surface area with HTT. With  $H_3PO_4$  treatment, there is no further increase in surface area above about 500°C. This may be due to the formation of inactive species (polyphosphates), or by structural rearrangement and associated contraction, if the crosslinks formed at low HTT have reached their limit of thermal stability.

As they are dominantly microporous, both series of carbons have high adsorptive capacities for small molecules (iodine number), but low capacities for larger molecules (methylene blue value). The KOH carbons have a higher capacity for phenol adsorption than the  $H_3PO_4$  carbons which cannot be explained on the basis of surface area alone. It is suggested that KOH activation produces carbons with more favorable surface chemistry.

## ACKNOWLEDGEMENTS

The authors wish to acknowledge the assistance of Danny Turner, Hengfei Ni and Bob Rathbone of the CAER. This work has been sponsored by the State of Kentucky and by the Illinois Department of Energy and Natural Resources through its Coal Development Board and Illinois Clean Coal Institute.

## REFERENCES

1. Derbyshire, F.J., Jagtoyen, M., McEnaney, B., Rimmer, S. M., Stencel, J. M., Thwaites, M. W., Proceedings 1991 ICCS Conference, 480-483, Newcastle, England, 16-20 September, 1991, Butterworth-Heinemann Ltd, 1991.
2. Derbyshire, F.J., Jagtoyen, M., McEnaney, B., Sethuraman, A. R., Stencel, J. M., Taulbee, D. and Thwaites, M.W., American Chemical Society, Fuel Division Preprints, 36 (3), 1072-1080, 1991.
3. Jagtoyen, M., McEnaney, B., Stencel, J. M., Thwaites, M.W. and Derbyshire, F. J., American Chemical Society, Fuel Division Preprints, 37 (2): 505-511, 1992.
4. Jagtoyen, M., Thwaites, M.W., Stencel, J. M., McEnaney, B. and Derbyshire, F.J., *Carbon*, 30 (7), 1089-1096, 1992.
5. Durie, R.A., Schafer, G.N.S. *FUEL*, 58, 472-476, 1978.
6. Guy, P.J., Verheyen, T.V., Felber, M.D., Heng, S., Perry, G., Australian Coal Science Conference, Brisbane, 380-386, 1990.
7. Wennerberg, A.N., Grady, T.M., United States Patent 4.082,694, 1978.
8. Audley, G. J., European Patent 0 312 395 A2, The British petroleum company p.l.c, 1989.
9. Gregg, S.J., Sing, K.S.W. in Adsorption, Surface Area and Porosity, 2nd ed., 94-100, Academic, London, 1982.
10. Rodriguez-Reinoso, F., Martin-Martinez, J. M., Prado-Burquette, C.P. and McEnaney, B., *J. Phys. Chem.*, 91, 515-516, 1987.
11. Friedman, S., Utz, B. R., Nowak, M. A., Fauth, D. J., Schmidt, C. E. "Base catalysed desulfurization and heteroatom elimination from coal-model heteroatomic compounds", 1987 International Conference on Coal Science, edited by J. A. Mouljin et al., Elsevier Science Publishers B. V., Amsterdam, 1987.
12. Verheyen, T. V., Derbyshire, F. J. and Jagtoyen, M., paper in preparation for Carbon.
13. Derbyshire, F.J., Jagtoyen, M., McEnaney, B., Rimmer, S.M., Stencel, J.M. and Thwaites, M.W., *Extended Abstracts, 20th Biennial American Conference*, 52-53, Sta. Barbara, Ca., 23-28 June, 1991.
14. Laine, J., Calafat, A. and Labady, M., *Carbon*, 27, 191-195, 1989.
15. Jagtoyen, M., Derbyshire, F. J., submitted for publication, 1993.
16. A. Cotton, G.Wilkinson, P. Gaus, *Basic Inorganic Chemistry*, 2. ed., John Wiley & Sons, New York, 1987.
17. Activated Carbon Evaluation and Selection, Autochem-Cecarbon, Tulsa, Oklahoma, 15-17.
18. CEFIC, Test Methods for Activated Carbons, European Council of Chemical Manufacturers Federations, 21-27, 1986.

Table 1: Composition of coals.

Coal	Av.P.Diam ( $\mu\text{m}$ )	Ash (%)	C	H	N	S	O
			(% daf basis)				
106	80	9.6	83.2	5.5	2.0	3.9	5.4
106clean	5	3.3	84.8	5.5	2.0	2.6	5.1

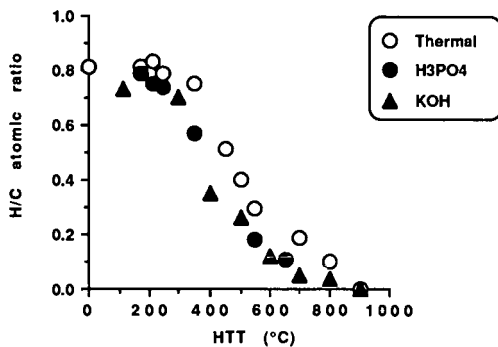


Figure 1: Change in H/C ratio for carbons synthesized from bituminous coals.

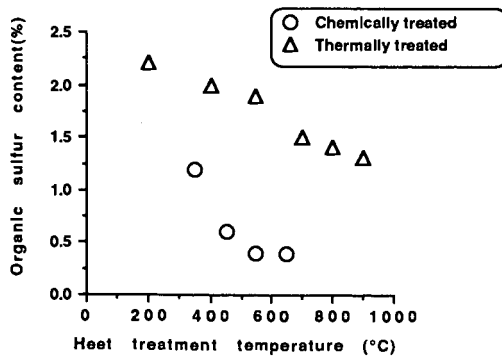


Figure 2: Organic sulfur removal is promoted by chemical treatment.

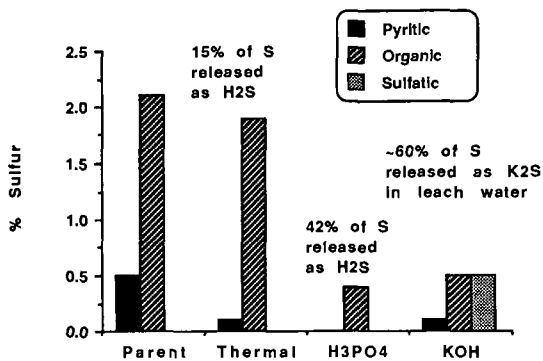


Figure 3: Mode of sulfur removal depends on type of treatment.

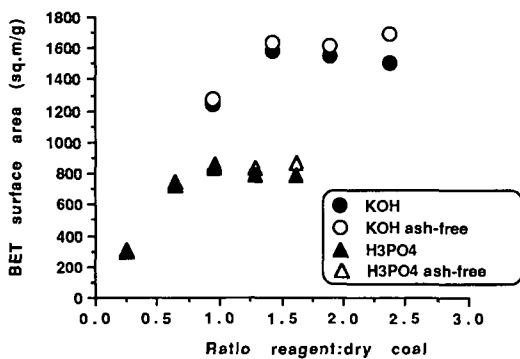


Figure 4: Ratio of reagent to precursor influences surface area (HTT: H3PO4, 500C; KOH, 800C)

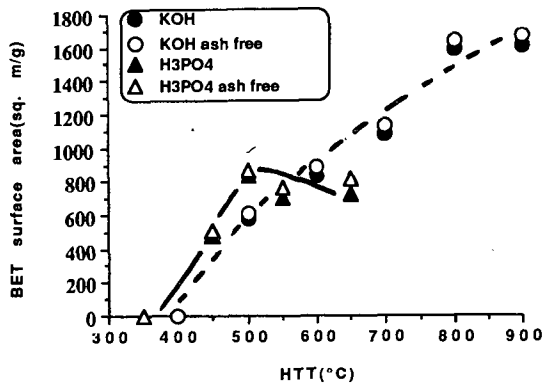


Figure 5: Surface area dependence upon HTT.

## TREATMENT OF ACTIVATED CARBONS FOR DENSIFICATION

Mark L. Stewart and John M. Stencel  
Center for Applied Energy Research  
University of Kentucky, Lexington, KY 40511

**Keywords:** Surfactant, densification, activated carbon

### ABSTRACT

Although activated carbons can have very high surface areas and micropore volumes, their adsorption capacity is generally achieved at the expense of density. Decreased density limits the applicability of carbons for adsorption storage of compressed natural gas and vehicular fuels, even though their potential use has been shown to offer advantages where storage volume is limited.

In this study, activated carbons were treated with surface active agents to increase their bulk and pressed densities. This treatment, along with a hydraulic pressing procedure, are described in which the carbon densities are enhanced without significant adverse effects on their adsorbent properties. It is also shown that surface active agent treatment decreases the work needed to densify the carbons and that specificity in densification is influenced by the ionic character of the agent. As a result, even higher volumes of adsorption storage is expected relative to untreated adsorbents, especially for carbons having very high surface areas ( $\sim 2000 \text{ m}^2/\text{g}$ ) and low densities ( $\sim 0.2 \text{ g/cc}$ ).

### INTRODUCTION

In general, the  $\text{N}_2$  adsorption surface areas of activated carbons are very high, and in the range  $600 - 2800 \text{ m}^2/\text{g}$ . As a consequence, they have inherently low densities ( $\sim$  or  $< 0.4 \text{ g/cc}$ ), and the amount or mass of carbon that can be accommodated in a limited volume is restricted. Ideally, a combination of high surface area, microporosity, and high density would be desirable for particular applications; for example, in the storage or adsorption of hydrogen, methane, or natural gas, it is imperative to maximize density while maintaining surface area and microporosity(1-4).

The purpose of this communication is to address the concept of densifying activated carbons produced from fossil resources with a surface active agent while maintaining reasonable levels of microporosity and adsorption capacity. The process uses low concentrations of inexpensive additives called surface active agents (surfactants) to enhance densification. These commercially available surfactants are anionic, cationic or amphoteric in nature and are interacted with activated carbons before or during densification processes that could be used in the carbons industry. This process was devised to enhance the density of activated carbon at a lower and more economical work input while maintaining inherent surface area and porosity in comparison to that obtained when using standard compaction, extrusion or pelletization without the addition of surface active agents.

## EXPERIMENTAL

Three commercial activated carbons were used in the study; they were supplied by Amoco Research and Development, Norit N. V. Activated Carbon, and Sutcliffe Speakman Carbons Ltd. The BET surface areas and densities for each carbon respectively are as follows: 2600 m<sup>2</sup>/g, 2000 m<sup>2</sup>/g, 850 m<sup>2</sup>/g and 0.18 g/cc, 0.21 g/cc, and 0.38 g/cc.

Two surfactants were used in the experiments and are classified as anionic and cationic in charge. These surfactants were dissolved into distilled de-ionized water with stirring at a temperature at which dissolution was rapid, ~ 50° C. Surfactant concentrations in the range 0 - 1.0% by weight were used, since at levels in excess of approximately 1.0% surfactant solubilities typically reach a critical point of saturation, thereby causing unwanted agglomeration and formation of micelles. The activated carbons were treated and then heated to approximately 50° C with stirring. This temperature is not a factor controlling the effects of the surfactant on carbon density, but rather enable it to uniformly deposit and interact with the carbon without causing excess water boil-off or surfactant decomposition. The solution-carbon mixture was then filtered and dried at temperatures of 100-200° C to remove excess water. As a control to verify the attributes of surfactant addition, each of the samples was also treated with only distilled, de-ionized water (i.e. 0% surfactant) using a procedure identical to that used for preparing surfactant treated samples.

Apparent density measurements of the carbons were obtained in accordance to ASTM procedure D-2854 (5). This procedure is commonly practiced in industry. Carbon samples are fed through a feed funnel into a 100 ml graduated cylinder. The apparent density is then calculated as grams of carbon per unit volume. Any mechanical or vibrational packing effects were minimized in an effort to measure true inherent apparent densities.

Secondly, the pressed density of the carbons were obtained through the use of a pressing/pelleting technique. In determining pressed density, a cylindrical stainless steel die was used with a hydraulic press to supply the pressure on a graduated plunger. A premeasured mass of activated carbon was compressed under a steadily increasing hydraulic force of 0 - 89,000 N. By using the cylindrical volume (V) relationship ( $V=4\pi r^2h$ , where r is the radius of the plunger and h is the height of compacted carbon in the die) the change in volume vs. pressure was obtained. The volume of the pressed carbons was calculated using predetermined hydraulic forces - 11,125, 22,250, 44,500, 66,750, and 89,000 N; and, at these forces, the density was calculated using the mass per volume relationship  $\rho=m/v$ , where m was the premeasured mass of the sample before pressing. In addition to the density measurements, work and force relationships were calculated using standard equations to look at potential ramifications of the procedure.

Surface area measurements were performed on the control and the surfactant treated samples to evaluate effects of the treatment on adsorption capacities. Standard nitrogen adsorption (6) using a static volumetric flow process was used, employing a Coulter Omnisorp 100CX sorption system. All surface areas were calculated using the standard BET equation between relative pressures of 0.05 - 0.25. All samples were pretreated under similar conditions to ensure uniformity in data interpretation.

## RESULTS AND DISCUSSION

Figure 1 displays the percent increase in apparent density relative to the standard data given in Table 1 for the carbons when treated with a 0.4 and 0.8% anionic surfactant. The maximum increase in apparent density is near 11% for the Norit activated carbon when using 0.8% by weight surfactant. The increased density of the 0.8% treated carbons suggests a cumulative effect which entails the ability to sufficiently cover the activated carbon surface with a minimum surface layer of surfactant. It has also been determined that treatments at concentrations of 1.0% or greater can cause decreased density in comparison to a 0.8% treatment. Hence, there is a maximum in density as a function of surfactant concentration rather than an increasing density with increasing surfactant concentration.

Using a cationic surfactant, the apparent density changes relative to the standard are displayed in Figure 2. The maximum increase in apparent density is 9% for the Amoco activated carbon when using a 0.8% surfactant treatment. The effects of cationic surfactant treatment are significantly different than the effect of the anionic surfactant treatment. This specificity is probably related to fundamental physical and chemical differences between the surfactants and their interaction with the carbons. This suggests possible inherent charge differences between the particles have been neutralized in the surfactant densification procedure. In addition, the data displayed in Figures 1 and 2 imply that a variable control of carbon density might be possible with either step-wise anionic/cationic treatments or amphoteric surfactants.

Figure 3 illustrates the work input needed to compact the Amoco activated carbon powder through a range of densities. The work-density plots for the Norit and A207 samples show similar behavior. Commercially it is imperative to increase carbon densities to maximize either the mass incorporated into a limited volume and/or to produce compacted pellets or extrudates which are resistant to decrepitation (1-4). Analysis of the data in Figure 3 show that the work required to achieve a particular density is significantly less for a sample that has been treated with surfactant. In the case of the Amoco activated carbon, the work input needed to compact the carbon to densities between 0.7-1.4 g/cc decreases by approximately 35% after treatment. This work input data implies that there is a potential and significant economic benefit to using surfactants during compaction, extrusion, or pelletization. It is also, however, imperative to retain specific or reactive surface area of the carbons if surfactant treatment is to be used during carbons processing.

Nitrogen BET surface areas of the pressed carbons are displayed in Figure 4. In general, the precision of the surface area measurement is (+/-) 5%. Within this precision limit, anionic and cationic surfactant treatments did not cause significant changes in the surface areas of the carbons. Surface area analysis on the carbon in their powdered, unpressed form showed similar results except for a marked decrease in surface area for the cationic treatments. Hence, the benefit of surfactants for powdered carbons, in which both density and surface area are considered, is dependent on the ionic character of the surfactant.

## CONCLUSIONS

Surfactant treatment has shown to be beneficial in the densification of high surface area activated carbons for potential natural gas storage applications. This simple and inexpensive procedure has been shown to increase the densities of activated carbons without significantly inhibiting their adsorption storage potential. For applications in which storage volume is limited at certain pressures, a combination of high density and porosity can be achieved through a combination of surfactant treatment and hydraulic pressing of activated carbons. It is known that activated carbons can contain either positively or negatively charged surfaces and that the magnitude of the charge can be influenced by chemical treatment of the carbon (7-10). In the examination of anionic and cationic surfactant treatments, it appears that selective neutralization and alteration of surface charge is surfactant dependent. The action of the surfactants in enhancing carbon density and in decreasing the work necessary to produce a densified carbon is therefore tentatively related to the elimination or minimization of surface charge.

## ACKNOWLEDGEMENTS

Appreciation is extended to Amoco Research and Development, Norit N. V. Activated Carbon and Sutcliffe Speakman Carbons Ltd. for supplying the activated carbon samples.

## REFERENCES

1. B. Buczek and L. Czepirski, *Adsorp. Science & Technol.*, **4**, 217(1987).
2. S.S. Barton, J. R. Dacey and D. F. Quinn, *Fundam. Adsorp.*, Proc. Eng. Found. Conf., (Ed. A. L. Myers, G. Belvort Eng. Found), 65(1983).
3. K. Otto, Adsorption of Methane on Active Carbons and Zeolites, (Hemisphere Publ. Corp.), **4**, 241(1982).
4. "Natural Gas Storage", D. F. Quinn and J. A. MacDonald, Proc., Workshop on Adsorbent Carbon, 6/20-21/91, Lexington KY.
5. Standard Test Method for Apparent Density of Activated Carbon, ASTM Committee D-28 - D2854-89, p. 329, (3/31/89).
6. S. Brunauer, P. H. Emmett, and E. Teller, *J.A.C.S.* **60**, 309(1938).
7. M. K. Abotsi Godfried and A. W. Scaroni, *Fuel Proc. Tech.* **22**, 107(1989).
8. V. A. Gareten and D. A. Weiss, *J. Chem.*, **10**, 309(1957).
9. B. R. Puri, Chemistry and Physics of Carbon, Vol. **6**, (Marcell Dekker, NY), Ed. P. L. Walker, 1970.
10. J. B. Donnet, *Carbon* **6**, 161(1968).

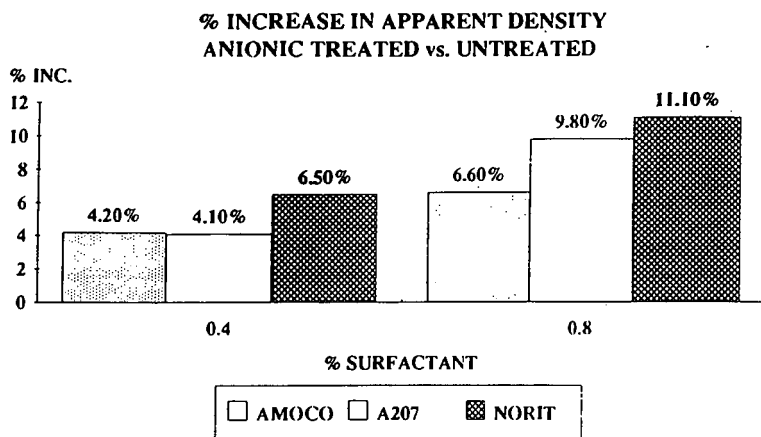


Figure 1.

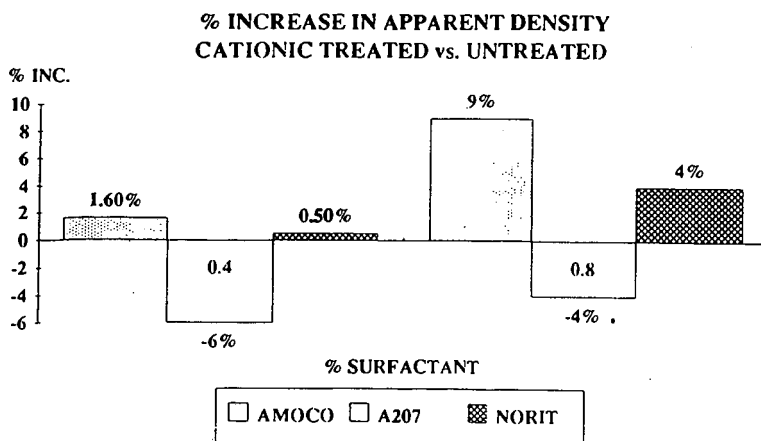


Figure 2.

**AMOCO ACTIVATED CARBON**  
**Work vs. Density**

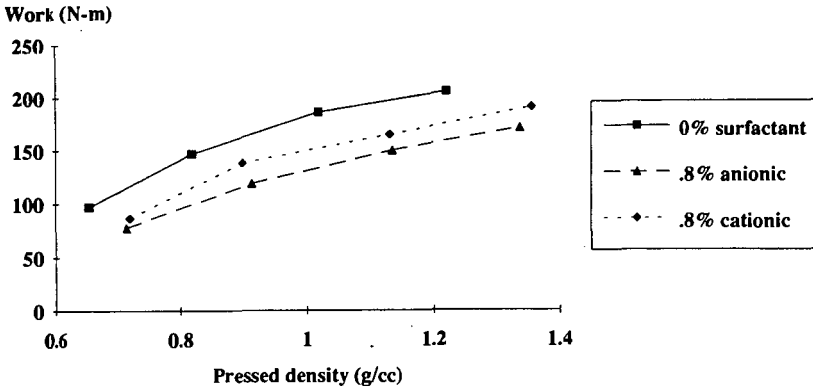


Figure 3.

**SURFACTANT TREATED PRESSED CARBONS**  
**BET SURFACE AREA**

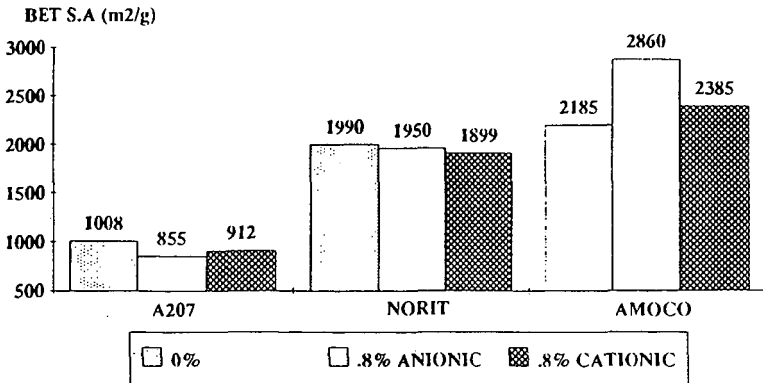


Figure 4.

## Formed Activated Carbons from Bituminous Coals by KOH Activation

Vincent Verheyen, Marit Jagtoyen\* and Frank Derbyshire\*

Coal Corporation of Victoria, PMB No.1 Morwell,  
3840 Australia

University of Kentucky, Center for Applied Energy Research,  
3572 Iron Works Pike, Lexington, KY 40511-8433

**Keywords:** activated carbon, potassium hydroxide, bituminous coal, nitric acid

### INTRODUCTION

Coals of various ranks are important precursors for the synthesis of activated carbons in powder, granular or extrudate forms. The commercial manufacture of carbons from bituminous coals generally involves carbonization followed by steam activation of the char to generate the required pore structure and surface area. Pitch binders can be used to produce hard pelletized products. Large size carbons have higher market value than powders, as they can be used in fixed bed adsorbers, allowing cyclic operation, and regeneration.

Low rank brown coals can be processed into pelletized highly microporous carbons using a different approach to that described above (1, 2). This involves alkaline digestion of the humic acid rich coal with potassium hydroxide to form an extrudable paste which can be carbonized and activated in a single heat treatment step, although a subsequent leaching step is required to recover the reagent. The KOH promotes both binding and chemical activation, and no further activation with steam or CO<sub>2</sub> is required. Even though KOH has been shown to be an effective chemical activant for producing powdered activated carbons from petroleum cokes and bituminous coals (3, 4), these precursors do not contain humic acids or sufficient acidic functional groups to enable their colloidal dissolution in aqueous KOH. Therefore the successful pelletization of bituminous coal/KOH mixtures is not normally possible without added binder.

To attempt to circumvent this difficulty, an approach has been taken in which bituminous coals are subjected to an oxidative pretreatment in order to modify the coal structure, remove mineral matter, enhance digestion in KOH, and induce strong binding properties. This paper describes an investigation of the effects of pre-oxidation with HNO<sub>3</sub> on the production and properties of pelletized activated carbons from bituminous coals using KOH. Nitric acid was chosen because of its known ability to oxidize coals (5, 6), and because it has the advantage over other strong oxidants such as Cr<sub>2</sub>O<sub>7</sub> in being able to generate humic acids in high yield (7,8). The research is germane to the diversification of use of coal resources, many of which face increasing environmental constraints on their direct utilization as fuels.

### EXPERIMENTAL

Western Kentucky No.9 seam (high vol.C) coal was dried, ground to minus 100 mesh, and oxidized by reaction with an aqueous solution of HNO<sub>3</sub> at concentrations from 0.25 to 2N. The reaction was conducted with vigorous stirring at 373K for 8 hours, or until visible signs of reaction had ceased. The oxidation product was filtered and washed with distilled water prior to drying.

Extrudable pastes were prepared by slowly blending the appropriate dry feedstock in a paddle mixer with a concentrated KOH solution. A KOH/fixed carbon ratio of 1:1 was maintained for all feedstocks. Sufficient water was added to prepare a paste of suitable consistency for extrusion. A low-pressure screw extruder, equipped with a multi-hole die, was used to prepare the spaghetti-like product. The extrudate was dried overnight at 353K to form hard brittle strands which were then roller crushed and sealed in moisture proof bags.

Both HNO<sub>3</sub> and HNO<sub>3</sub>/KOH treated feedstocks were carbonized in a N<sub>2</sub> purged tube furnace which was temperature programmed from ambient to 1173K at 15K/min., with a 60 min. dwell at the maximum temperature. After cooling, the product was water washed, boiled with a 5% HCl soln. to remove excess potassium, and dried. Proximate analyses were obtained using a LECO-MAC 400.

Information on the carbon pore structure was derived from nitrogen adsorption isotherms obtained at 77K on a Coulter Omnisorb 100CX apparatus; the micropore volume W<sub>0</sub> was determined using the Dubinin-Raduskevich equation (9). The average width of slit shaped pores was determined using the expression suggested by Stoekli et al. (10), which is valid for pores of diameter 0.45-2.5 nm;

$$L(\text{nm})=30/E_0+5705/E_0^3+0.028E_0-1.49$$

Specific surface areas, S<sub>BET</sub>, were obtained from the adsorption isotherms using the BET equation.

Non-microporous surface areas, S'<sub>BET</sub>, and micropore volumes were obtained using the α<sub>s</sub> method (11); standard isotherm data were taken from Rodriguez-Reinoso et al. (12).

Relative carbon hardness was estimated using the Takeda microstrength hardness test method (13). Fourier transform infrared (FTIR) spectra of the HNO<sub>3</sub> treated coals were obtained from 0.4% loaded KBr discs using a Nicolet 20SX spectrophotometer.

## RESULTS AND DISCUSSION

Nitric acid oxidation of the coal produced an expected decrease in ash content, due to leaching the acid-soluble minerals, Table 1(a). However, treatment with 0.25N and 0.5N HNO<sub>3</sub> did not remove all of the pyrite present in the coal, as the remaining pyrite separated from the lower density oxidation products during water washing. At low HNO<sub>3</sub>/coal ratios the fixed carbon content of the oxidation products increased above that reported for the coal. This may indicate that, under conditions of moderate oxidation, products are generated that participate in thermally induced condensation reactions, resulting in a net increase in fixed carbon content. The test to determine the fixed carbon content provides conditions under which such reactions can take place. With more severe oxidation, there was a reduction in fixed carbon as, presumably, the increased oxygen content of the coal contributed to the loss of carbon as volatile products.

The FTIR spectra presented in Figure 1 reveal a progressive increase in the intensity of acidic hydroxyl (broad 3700-2400 cm<sup>-1</sup>), carbonyl/carboxyl (~1700 cm<sup>-1</sup>) and NO<sub>2</sub> (1547cm<sup>-1</sup>) absorption bands with increasing severity of HNO<sub>3</sub> treatment. Interestingly, the spectra of the 1N and 2N HNO<sub>3</sub> oxidation products are comparable to those of untreated lignites or brown coals, such as Beulah (North Dakota, USA) and Loy Yang (Victoria, Australia), indicating that the acid treatment may have the desired result of effectively lowering the coal rank. The absorption bands associated with clays/silicates are unaffected by the HNO<sub>3</sub> treatment, while the intensities of the bands associated with aliphatic absorbance (~2900cm<sup>-1</sup> and 1450cm<sup>-1</sup>) decrease with increasing oxidation severity. However, the loss of aliphatic structure may be exaggerated by changes in the infrared extinction coefficients.

Thermal treatment of the  $\text{HNO}_3$  oxidized coals produced yields of char, Table 1(b), that were somewhat higher than the fixed carbon contents of the starting materials. Due to the loss of volatile matter on heat treatment, there was a general increase in ash content with oxidation severity.

The presence of KOH during heat treatment produced carbons with consistently lower yields than the corresponding thermal products, and these decreased with increasing oxidation severity, Table 1(c). Despite the lower carbon yields, the ash contents are reduced, rather than being further concentrated by the loss of carbonaceous material. Obviously, reaction with KOH converts some of the coal mineral constituents to soluble products that are removed upon product washing. Similar effects have been found in studies of the KOH activation of powdered bituminous coal (4).

Calculations based on the fixed carbon content, Table 1(b) and (c), show that fixed carbon is lost during KOH activation of the coals subjected to mild oxidation. In contrast, KOH activation of the more severely oxidized feedstocks results in negligible loss of fixed carbon during thermal treatment. Unpublished research has shown that no significant fixed carbon burnoff occurs on the activation of brown coal/KOH pellets (14). These observations suggest that the loss of fixed carbon during chemical activation by KOH exhibits an inverse rank dependence, with the more severely oxidized bituminous coals behaving similarly to low rank coals.

The nitrogen adsorption isotherm data presented in Table 2 reveal that  $\text{HNO}_3$  oxidation decreases the already low surface area and pore volume of the bituminous coal feedstock. Thermal treatment also produces solid products with negligible porosity. These results contrast with the well established ability of  $\text{HNO}_3$  to regenerate spent activated carbons (15).

On the other hand, the activated carbons produced with KOH reveal that even low levels of  $\text{HNO}_3$  oxidative pretreatment have a marked effect on the generation of microporosity, Table 2. At the lowest level of oxidation, the BET surface area increases by over 30% and the micropore volume by about 75%. Increasing the severity of oxidation further enhances the development of surface area and micropore volume, which are increased by over 50% and 100% respectively, after treatment with 2.0N  $\text{HNO}_3$ . The increase in surface area and pore volume of these carbons may help to explain their lower ash yields, since the high porosity will allow greater access during acid washing, leading to the more effective removal of soluble ash constituents.

The relative microstrength hardness of the active carbons is presented in Figure 2 along with some commercial carbons for comparison. The feedstocks and chars produced from the parent coal and after 0.25N  $\text{HNO}_3$  oxidation did not form extrudable mixtures with KOH. At higher oxidation levels, the extent of reaction and dissolution in the KOH solution was found to increase with severity of treatment. The reaction between the 1N and 2N  $\text{HNO}_3$  oxidation products and KOH was strongly exothermic with some  $\text{NH}_3$  evolution. These mixtures behaved like colloidal gels and were readily extruded. A dramatic increase in product carbon hardness was found on going from 0.5N to 1N  $\text{HNO}_3$  oxidation. Oxidation with 2N  $\text{HNO}_3$  improved the carbon hardness above that determined for commercial bituminous coal-derived activated carbons.

## SUMMARY

The pretreatment of bituminous coals by nitric acid oxidation produces a feedstock that, in the presence of KOH, is suitable for extrusion and for the synthesis of hard, high surface area activated carbons. Nitric acid serves several roles in the formation of pelletized carbons from bituminous coal:

- (1) it reduces the ash content,
- (2) it introduces sufficient acidic functionalities, including regenerated humic acids, to the

coal to enable dissolution in KOH solution, conferring binding properties for the formation of hard, shaped carbon precursors: the strength is retained during heat treatment, and

(3) it increases the ability of the KOH to generate microporosity.

#### REFERENCES

1. Guy, P.J.; Perry, G.J. *Fuel* 1992, **71**, 1083.
2. Guy, P.J., Verheyen, T. V., Heng, S., Felber, M. D. and Perry, G. J., *Proc. Int. Conf. Coal.Sci.* 1989, 23.
3. Marsh, H., Crawford, D., O'Grady, T. M. & Wennerberg, A., *Carbon* 1984, **22**,603.
4. Derbyshire, F.; Jagtoyen, M., "Synthesis of Adsorbent Carbons from Illinois Coals", Final Technical report to ICCI, August 31st., 1992.
5. Lowry, H.H. *J.Inst.Fuel* 1937, **10**, 294
6. Lilly, V.G.; Garland, C.E. *Fuel* 1932, **11**, 392.
7. Yohe, F.R.; Harman, C.A. *Trans.Illinois State Ac.Sci.* 1939, **32**, 134.
8. Lowry, H.H.(ed)*Chemistry of coal utilization.*Vol 1.1945, 358.
9. Dubinin, M. M. Zaverina, E. D. and Raduskevich, L. V. *Zh. Fiz. Khimii* , 1947, 1351.
10. Stoekli, H.F, Ballerini, L. De Bernadirmi, S., *Carbon*, 1989, **27**, 501.
11. Gregg, S.J.; Sing, K.S.W. *Adsorption, Surface Area and Porosity.* 2nd ed. 1982, 98.
12. Rodriguez-Reinoso, F., Martin-Martinez, J. M., Prado-Burquette, C.P. and McEnaney, B., *J. Phys. Chem.*, 1987, **91**, 515.
13. Takeda Chemical Industries Ltd (Japan). *Bulletin: Test procedures for activated carbon*, 1973.
14. Coal corporation of Victoria, internal reports.
15. Mueller, G., Ramsteiner, R., Graf, F. and Hupfer, L., *Fed. Rep. Ger. Patent DE 3536263 A1*, April, 1987.

#### ACKNOWLEDGEMENTS

T. V. Verheyen acknowledges the exchange visitors program between the Coal Corporation of Victoria and University of Kentucky, Center for Applied Energy Research that made this research possible.

Table 1: Analysis of HNO<sub>3</sub> treated coals and heat treated products.

(a) oxidized coal

HNO <sub>3</sub> Normality (W/W)	HNO <sub>3</sub> /Coal Ratio	Ash	Volatiles	Fixed Carbon
		dry basis		
0	-	14.48	36.00	49.52
0.25	0.22	7.60	36.05	56.35
0.5	0.44	6.87	37.07	56.06
1.0	0.88	5.66	44.89	49.46
2.0	1.76	5.93	56.06	38.01

(b) Thermally treated coals(1173K)

HNO <sub>3</sub> Normality	Yield (%w/w)	Fixed C Yield (%w/w)	Ash	Volatiles	Fixed Carbon
			dry basis		
0.0	66	110	11.17	2.33	86.50
0.25	69	107	8.73	2.29	88.97
0.5	59	95	8.77	<.1	91.18
1.0	55	98	7.98	2.41	89.61
2.0	52	117	9.94	3.29	86.77

(c) KOH activated coals (1173K; 1:1 KOH:Fixed Carbon)

HNO <sub>3</sub> Normality	Yield (%w/w)	Fixed C Yield (%w/w)	Ash	Volatiles	Fixed Carbon
			dry basis		
0.0	54	83	5.02	7.91	87.07
0.25	53	84	3.73	8.60	87.67
0.5	52	81	5.83	7.18	86.98
1.0	49	95	4.65	5.84	89.51
2.0	45	108	4.01	3.26	92.73

**Table 2: Nitrogen Adsorption Isotherm Data**

(a): BET surface area of feedstocks and thermally treated coals (1173K)

HNO <sub>3</sub> Normality	BET Surface Area (m <sup>2</sup> /g <sup>-1</sup> )	
	Feedstocks	Thermally treated
0	21	2
0.25	6	1
0.5	2	1
1.0	6	4
2.0	1	11

(b): Activated Carbons

HNO <sub>3</sub> Normality	Micropore Volume (cm <sup>3</sup> g <sup>-1</sup> )	BET Surface Area (m <sup>2</sup> g <sup>-1</sup> )	Mean Pore Width Angstrom	Mesopore Surface Area (m <sup>2</sup> g <sup>-1</sup> )
0	0.37	1035	-	36.6
0.25	0.65	1374	7.08	69.6
0.5	0.72	1473	7.63	38.1
1.0	0.71	1517	6.08	34.8
2.0	0.74	1602	7.13	52.2

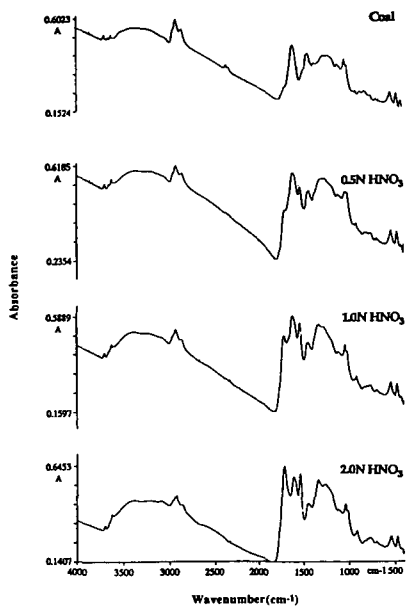


Figure 1: FTIR spectra of Western Kentucky No.9 bituminous coal and its solid HNO<sub>3</sub> oxidation products

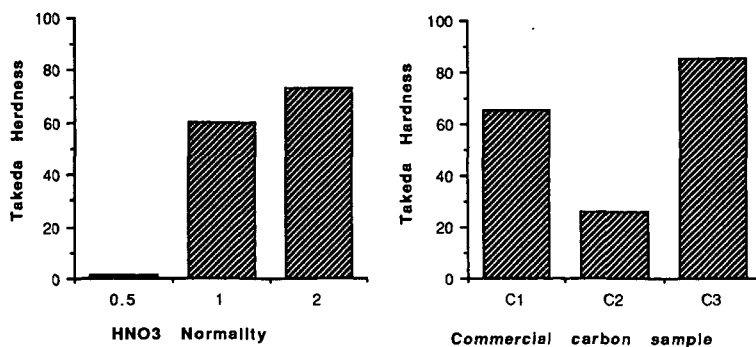


Figure 2: Takeda hardness of activated carbons and commercial samples. (C1 and C2: bituminous coal derived, C3: coconut shell derived)

## SO<sub>2</sub> AND NO<sub>x</sub> REMOVAL AT AMBIENT TEMPERATURES USING ACTIVATED CARBON FIBERS

S. Kisamori, S. Kawano, I. Mochida,  
Institute of Advanced Material Study, Kyushu University  
Kasuga, Fukuoka, 816 Japan.

Key words: SO<sub>2</sub> removal, NO<sub>x</sub> reduction, Activated Carbon Fiber(ACF)

### Abstract

The activity of polyacrylonitrile (PAN) and pitch based activated carbon fibers (ACF) has been studied for the removal of SO<sub>2</sub> and the reduction of NO<sub>x</sub> from air at ambient temperatures. The PAN-ACF was found to be active for oxidizing SO<sub>2</sub> and hydrating the product of H<sub>2</sub>SO<sub>4</sub>. The acid flows down from the ACF bed, maintaining the activity for SO<sub>2</sub> removal, and allowing the acid to be recovered. The influences of temperature, humidity, and contact time on the rate of SO<sub>2</sub> removal will be presented.

The pitch-ACF, when further activated with H<sub>2</sub>SO<sub>4</sub> at 400°C, was found to remove NO<sub>x</sub> at low concentrations (around 10ppm) by reaction with NH<sub>3</sub> at temperatures around 10°C and at 100% humidity. Heating the air to reduce the relative humidity was found to effectively enhance activity. Further, heat treatment of the fibers in inert atmosphere before activation enhanced the activity under high humidity. The cause of catalytic activity in the ACFs will be discussed.

### Introduction

In spite of extensive efforts to keep the atmosphere clean, acid rain problem is still growing globally. Extensive and efficient removal of SO<sub>x</sub> and NO<sub>x</sub> from the atmosphere as well as flue gas is strongly wanted to be developed.

The present authors have been involved in the dry removal of SO<sub>x</sub> and reduction of NO<sub>x</sub> with NH<sub>3</sub> using activated carbon fibers (ACF). SO<sub>x</sub> in the flue gas was oxidatively adsorbed as H<sub>2</sub>SO<sub>4</sub> on ACF at 100–150°C until its saturation, and was reductively recovered in concentrated SO<sub>2</sub>, consuming C of ACF as CO<sub>2</sub> to regenerate the adsorption ability of ACF. Such a deSO<sub>x</sub> has been commercialized with cheaper active coke, and polyacrylonitrile based ACF (PAN-ACF) exhibited very high capacity to reduce the volume of the reactor. However, the adsorption-recovery/regeneration sequence consumption of not cheap C, and large volume of reactor may prohibit current application.

NO<sub>x</sub> in flue gas has been found to be reduced with NH<sub>3</sub> on active coke at 120°C. Hence the deSO<sub>x</sub> and deNO<sub>x</sub> has been performed on the same coke in the three moving bed sequence of deSO<sub>x</sub>, recovery/regeneration and deNO<sub>x</sub>. However, the catalytic activity is not satisfactory especially at ambient temperatures. ACFs were found very active for this reaction.

In the present study, removal of SO<sub>2</sub> to be recovered in H<sub>2</sub>SO<sub>4</sub> and reduction of NO<sub>x</sub> in low concentration (≈10ppm) were both examined at ambient temperatures (0–80°C) using PAN-ACF and pitch based ACF (pitch-ACF), respectively. Very simple cleaning of atmosphere can be performed by very handy ways.

### Experimental

#### SO<sub>2</sub> removal

The SO<sub>2</sub> removal was carried out in the fixed bed flow reactor at 100, 80, 50, and 30°C using PAN-ACF as the catalyst. Its analysis is summarized in Table 1. The reactant gas contained 1000ppm SO<sub>2</sub>, 5% O<sub>2</sub>, 10, 20, and 30% H<sub>2</sub>O and the balance N<sub>2</sub>. The weight of ACF and total flow rate were 0.5 g and 100 ml, respectively. The SO<sub>2</sub> concentration in inlet and outlet gases were analyzed by a flame photometric detector.

#### NO<sub>x</sub> reduction

A pitch based active carbon fiber (OG-5A) was supplied from Osaka Gas in a yarn form. OG-5A was further activated with 12N-H<sub>2</sub>SO<sub>4</sub>(300 wt%) through impregnation, drying, and heat-

treatment up to 400°C for 4 h (abbreviated as OG-5A 3/400/4). The ACF was further activated with H<sub>2</sub>SO<sub>4</sub> under the same conditions. The analysis and surface areas of the as-received and further activated ACF are also summarized in Table 1.

Reduction of NO with NH<sub>3</sub> was performed in a fixed bed U-shaped flow type reactor. The weight and length of fiber bed, flow rate, the concentrations of NO and NH<sub>3</sub> in air, and reaction temperatures were 0.5 g, 70 mm, 50 ml·min<sup>-1</sup>, 10–400 ppm, 10–400 ppm, and 0–30°C, respectively. Air was humidified at the reaction temperature or some temperatures lower by 5 to 25°C than the reaction temperature. Reactant and product gases were analyzed by NOx meter (ECL-77A, YANAGIMOTO Co.,Ltd.).

## Results

### Capture of SO<sub>2</sub> in recoverable H<sub>2</sub>SO<sub>4</sub>

Figure 1 illustrates the capture profile of SO<sub>2</sub> in an atmosphere of 5% O<sub>2</sub>, 10% H<sub>2</sub>O on PAN-ACF at a temperature range of 30–100°C. W/F of this series of runs in the figure was 5×10<sup>-3</sup> g·min·ml<sup>-1</sup> (SV≈3000h). At 100°C, SO<sub>2</sub> was completely removed for 5h on the ACF and then broke through completely after 11h. Under the conditions, the desulfurization process is obligated to consist of capture, and recovery/regeneration steps. A lower temperature of 80°C prolonged the period of complete removal of SO<sub>2</sub> until 9h when SO<sub>2</sub> in the outlet gas started to increase gradually to reach 65% of the inlet concentration at 27h and stayed at this concentration until at least 45h.

Aq. H<sub>2</sub>SO<sub>4</sub> was found to fall down from the vertical reactor to be stored in the reservoir placed below the reactor. A further lower temperature of 50°C further prolonged the period of complete removal to 11h, delayed the increase of SO<sub>2</sub> concentration and reduced the stationary concentration after 45h to 35%. An ambient temperature of 30°C allowed complete removal up to at least 60h. The SO<sub>2</sub> concentration while its complete removal was as low as 10 ppm at highest.

Figure 2 illustrates the influences of humidity on the removal of SO<sub>2</sub> at 100°C and 80°C. Higher humidity favored the deSO<sub>x</sub> by prolonging the period of complete removal and enhanced the stationary removal. Humidity of 20% allowed 20% stationary removal at 100°C. Lower temperatures emphasized the influences. Humidity of 20 and 30% provided 40 and 90 % stationary removal of SO<sub>2</sub> at 80°C respectively. At 50°C, complete removal could continue by humidity of 20% until at least 60h.

Figure 3 illustrates SO<sub>2</sub> removal at various W/F at 30°C. W/F of 5.0×10<sup>-3</sup> g·min·ml<sup>-1</sup> allowed complete removal of SO<sub>2</sub> when humidity was fixed at 10%. A half value of W/F reduced the removal to 90%, indicating catalytic process of SO<sub>2</sub> oxidation and hydration on the ACF.

### Reduction of NO<sub>x</sub> on a pitch ACF and its activated ones

Figure 4 illustrates NO conversion at 22°C over a pitch (OG-5A) and its activated ones with H<sub>2</sub>SO<sub>4</sub>. The as-received ACF (Figure 4-1) provided a NO conversion of 50% at the start of the reaction, however the conversion decreased very rapidly to zero before 5h after the reaction started. Adsorption of NO is suspected. Activation of the ACF with H<sub>2</sub>SO<sub>4</sub> increased the conversion very significantly (OG-5A-S(3/400/4) Figure 4-2) the stationary conversion after the rapid decrease with in 5h was as high as 60%.

Humidity in the feed gas retarded the reaction very significantly, as shown in Figure 4-3. The stationary conversion on OG-5A-S(3/400/4) in 100% humidity decreased 15%, which was, however, nontrivial.

Figure 5 illustrates influences of humidity on NO reduction at 22°C. Pitch ACFs all activated with sulfuric acid lost severally the activity by increasing humidity. It is noted that an ACF of higher surface area appeared to provide lower catalytic activity.

### Heattreatment of ACFs

Influences of heattreatment to control the surface oxygen functional groups on ACF were examined on the NO<sub>x</sub> reduction. As shown in Figure 4, the heattreatment at 800°C (H-800) is very significant to provide an excellent conversion of 40% in dry air and 25% in wet air. Activation with H<sub>2</sub>SO<sub>4</sub> (S(3/400/4)) of the heattreated ACF was also significant to provide conversions of 70% in dry air and 40% in wet air. The heattreatment at this temperature to the H<sub>2</sub>SO<sub>4</sub> activated

ACF was interesting. The conversion in dry air decreased to 50% from 60%, but the conversion in wet air increased to 35% from 12%. Small retardation by humidity on the heat-treated ACF is also shown in Figure 5.

#### Discussion

##### SO<sub>2</sub> removal

The present study succeeded to capture SO<sub>2</sub> and recover it in H<sub>2</sub>SO<sub>4</sub>. The PAN-ACF showed excellent activity to oxidize and hydrate SO<sub>2</sub> and to push H<sub>2</sub>SO<sub>4</sub> flow down through its bed. PAN-ACF is very unique to show such a high oxidation activity very probably through its oxygen and nitrogen surface functional groups. Their cooperation may increase the oxidation activity. Humidity appeared very essential for the present process. Hydration of SO<sub>2</sub> and some dilution of H<sub>2</sub>SO<sub>4</sub> may be keys to allow H<sub>2</sub>SO<sub>4</sub> to flow down. Surface functional groups on ACF should interact with H<sub>2</sub>O vapor. Hence their control may allow the smaller humidity for the recovery of H<sub>2</sub>SO<sub>4</sub>.

##### NO<sub>x</sub>

The ACF surface can activate NO<sub>x</sub> and NH<sub>3</sub> at the same time to reduce the former into N<sub>2</sub>, as discussed in previous papers. The major concept in the present study is related to the retardation of water vapor which certainly inhibits adsorption of NO. At temperature above 100°C, such a retardation is rather negligible but becomes distinct at room temperature probably because of the high coverage by condensation. Hence hydrophobic pitch ACF is effective. Its heat treatment may delicately control the surface functional groups to enhance the catalytic activity. In previous papers, the authors emphasized the importance of NH<sub>3</sub> adsorption in the NO-NH<sub>3</sub> reaction since adsorption of NH<sub>3</sub> is slightly disturbed with water vapor. However, the heat treatment enhances the activity in spite of a significant decrease of NH<sub>3</sub> adsorption. Activation of NO should be emphasized, although active sites for NO are not clarified yet. In conclusion, PAN-ACF and pitch ACF are found very useful to capture SO<sub>2</sub> and reduce NO at ambient temperatures. Their practical application appears feasible.

Table 1 Profiles of ACFs

	Elemental Analysis(%)						Surface area
	C	H	N	O	S	Ash	(m <sup>2</sup> /g)
FE-300	78.1	1.4	4.5	16.0	-	0.3	1141
OG-5A	92.3	1.0	0.8	5.6	tr.	0.3	680
OG-5A(3/400/4)	80.0	1.5	0.7	16.1	0.7	1.0	770

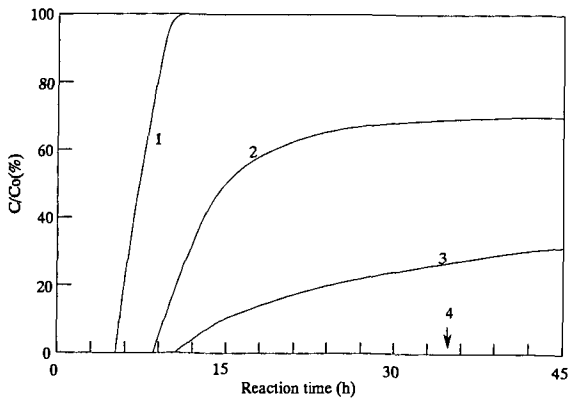


Fig.1 Breakthrough Profiles at Several Temperatures  
 $SO_2$  1000ppm,  $O_2$  5%,  $W/F=5.0 \times 10^{-3} g \cdot min \cdot ml^{-1}$

- 1 : 100°C
- 2 : 80°C
- 3 : 50°C
- 4 : 30°C

No.4 adsorbed  $SO_2$  completely at least 60 hours

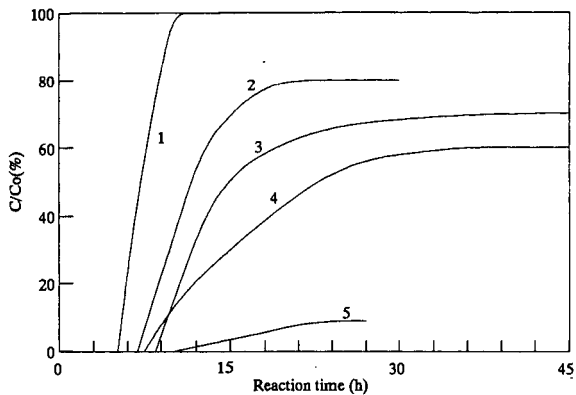


Figure.2 Influence of H<sub>2</sub>O Concentration for SO<sub>2</sub> Removal  
 SO<sub>2</sub> 1000ppm, O<sub>2</sub> 5%, W/F=5.0 × 10<sup>-3</sup> g · min · ml<sup>-1</sup>

- 1 : 100°C, H<sub>2</sub>O 10%
- 2 : 100°C, H<sub>2</sub>O 20%
- 3 : 80°C, H<sub>2</sub>O 10%
- 4 : 80°C, H<sub>2</sub>O 20%
- 5 : 80°C, H<sub>2</sub>O 30%

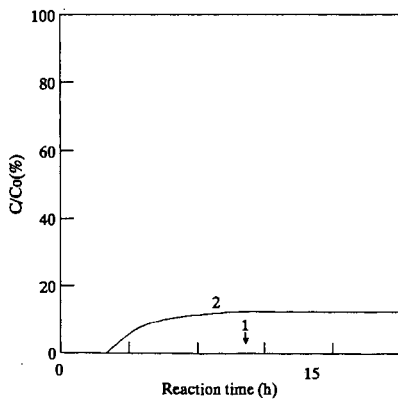


Fig.3 Effect of W/F for SO<sub>2</sub> Removal at 30°C  
 SO<sub>2</sub> 1000ppm, O<sub>2</sub> 5%, H<sub>2</sub>O 10%

- 1 W/F=5.0 × 10<sup>-3</sup> g · min · ml<sup>-1</sup>
- 2 W/F=2.5 × 10<sup>-3</sup> g · min · ml<sup>-1</sup>

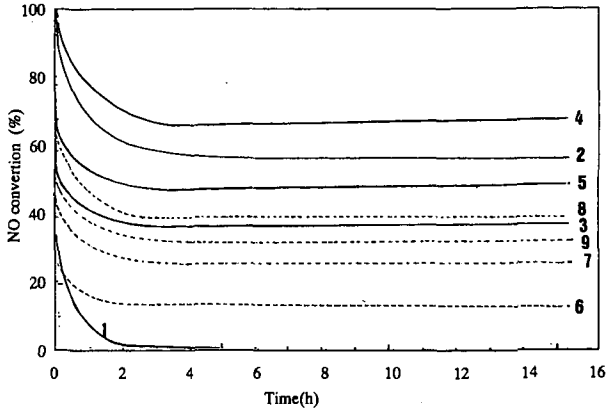


Figure 4 Conversion of NO in dry and wet air at room temperature over ACFs further activated with H<sub>2</sub>SO<sub>4</sub>

NO 10ppm, NH<sub>3</sub> 20ppm, W/F =  $5 \times 10^{-3} \text{g} \cdot \text{min} \cdot \text{ml}^{-1}$   
Temp. : 22°C

Dry air (r.h.:0%)

Wet air (r.h.:100%)

- |                             |                             |
|-----------------------------|-----------------------------|
| 1 : OG-5A                   | 6 : OG-5A-(300/400/4)       |
| 2 : OG-5A-(300/400/4)       | 7 : OG-5A-H800              |
| 3 : OG-5A-H800              | 8 : OG-5A-H800-S(300/400/4) |
| 4 : OG-5A-H800-S(300/400/4) | 9 : OG-5A-S(300/400/4)-H800 |
| 5 : OG-5A-S(300/400/4)-H800 |                             |

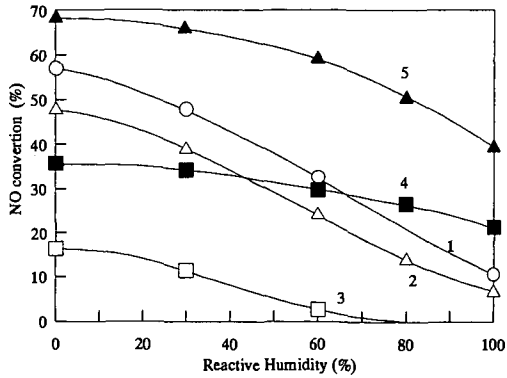


Figure 5 Stationary NO conversion vs. relative humidity(r.h)

Stationary conversion was observed at 15h after the reaction  
NO 10ppm, NH<sub>3</sub> 20ppm, W/F =  $5 \times 10^{-3} \text{g} \cdot \text{min} \cdot \text{ml}^{-1}$   
Temp. : 22°C

- |                     |                           |
|---------------------|---------------------------|
| 1 : OG-5A(3/400/4)  | 4 : OG-5A-H800            |
| 2 : OG-10A(3/400/4) | 5 : OG-5A-H800-S(3/400/4) |
| 3 : OG-20A(3/400/4) |                           |

## **CARBON FIBERS AND ACTIVATED CARBON FIBERS FROM RESIDUAL SHALE OIL**

**You Qing Fei, Frank Derbyshire and Thomas Robl**

**University of Kentucky, Center for Applied Energy Research,  
3572 Iron Works Pike, Lexington, KY 40511-8433**

**Keywords:** Carbon fibers, Activated carbon fibers, Shale oil

### **Introduction**

Oil shale is one of the largest fossil fuel reserves, and an important potential source of liquid fuels and chemicals. One of the disadvantages of oil shale liquids is their high nitrogen content, which causes difficulties in their upgrading to premium quality products[1]. To accentuate the problem, the nitrogen-containing species tend to be more concentrated in the higher boiling fractions of the retorted product [2]. An alternative solution may lie in investigating the use of the residual liquids as precursors for the synthesis of high added-value advanced carbon materials. The ability to generate valuable by-products could enhance the economics of oil shale retorting.

Carbon fibers (CF) and activated carbon fibers (ACF) are commercially produced from polyacrylonitrile (PAN) and petroleum and coal-tar pitches. The PAN-based fibers have very high strength for which reason they command a higher price than pitch-based ones. Other factors that contribute to the price are the high raw material cost, and low yield [3]. Pitch-based fibers can be formed by directly processing the precursor, to produce moderate strength isotropic carbon fibers, or after heat treatment to induce mesophase formation, when the fibers can have high modulus, and high thermal and electrical conductivity [4].

Activated carbon fibers produced from PAN have several unique properties[5], including the ability to adsorb NO<sub>x</sub>, SO<sub>x</sub> and vitamin B12[6,7], and where there may be novel metal-support interactions[8]. This may be related to their nitrogen content, which can lead to the presence of basic functional groups on the adsorptive surface. For similar reasons, it is considered that carbon fibers and activated carbon fibers produced from oil shale residues might exhibit unusual properties that are not possessed by fibers from petroleum or coal tar pitches. Accordingly, a program of work has been initiated to study the synthesis of carbon fibers from residual oil shale liquids.

In the study presented here, an asphaltene fraction was isolated from a shale oil residuum produced by the Kentort II process[9]. The fraction was processed by melt spinning, oxidative stabilization, carbonization and activation to produce carbon fibers and activated carbon fibers. The products were characterized by SEM, elemental and surface area analyses.

### **Experimental**

A shale oil residue (SOR), produced in the Kentort II process from eastern oil shale[9], was used as the starting material. The asphaltene fraction, SOR-AS, (hexane insoluble, benzene soluble) was separated as follows. The hexane soluble fraction of the shale oil residue was removed by extraction

with boiling hexane[10]. The hexane insoluble fraction was then Soxhlet extracted with benzene, following which the benzene was removed from the extract by rotary evaporation. A petroleum-derived isotropic precursor pitch (PP) was selected for comparison.

Continuous single filament carbon fibers were produced from the shale oil asphaltenes and the petroleum pitch by melt spinning, using a spinneret (capacity about 8g, nozzle diameter 0.3 mm) that is operated under nitrogen pressure. The shale oil and petroleum precursors were spun under 150–300 kPa pressure at about 240 and 300°C, respectively. The resulting fibers were then chopped into 15–20 mm lengths and stabilized by oxidation in air for 90 minutes at 180 and 230°C for the shale oil and petroleum pitch fibers, respectively. The stabilized fibers were carbonized in nitrogen at 850°C for 30 minutes. Carbon fibers were activated by reaction at 850°C for 60 minutes in 50 vol% steam or carbon dioxide, in nitrogen. The sequence of process steps for the preparation of carbon fibers (CF) and activated carbon fibers (ACF) is shown in Figure 1.

The morphology of the carbon fibers and activated carbon fibers was studied at magnifications up to  $\times 10^4$  by SEM (Hitachi S-2700). The BET surface area of activated fibers was measured by nitrogen adsorption at 77K, using a Quantachrome Autosorb 6.

## Results and Discussion

### Carbon Precursors

Analyses of the shale oil residue, its asphaltene fraction, and the petroleum pitch are shown in Table 1. The asphaltenes represent about 20 wt% of the original residue. It can be seen that the slightly higher nitrogen content of the residue (compared to the petroleum pitch) is considerably concentrated in the asphaltene fraction. The sulfur contents of the three materials are similar, but the petroleum pitch has a somewhat lower ash content. The shale oil asphaltene fraction has a softening point of 183°C, which is lower than that of the petroleum pitch, consistent with its higher hydrogen content.

### Carbon Fibers

Carbon fibers were successfully produced from the shale oil asphaltene fraction. SEM micrographs of the carbonized fibers are shown in Figure 2. Small particles (100–500 nm) were observed on the fiber surfaces: their origin is tentatively ascribed to the ash components in the precursor.

The form of the fibers was clearly retained after carbonization, indicating that the conditions chosen for stabilization were sufficient. The stabilization temperature of 180°C used here is much lower than those for conventional isotropic or mesophase pitches[11]. This suggests that the precursor have a very high oxidation reactivity.

While the freshly spun fibers had similar diameters for both precursors, the diameter of the shale oil carbonized fibers was smaller (in the range of 5–12  $\mu\text{m}$ ) than that of petroleum-derived ones (6–15  $\mu\text{m}$ ), as shown in Table 2. The greater degree of contraction of the shale oil fibers reflects their lower carbonization yield (50% versus 71%), or higher volatile matter content.

### ***Activated Carbon Fibers***

The morphology of activated carbon fibers derived from petroleum pitch and shale oil asphaltenes, and produced by activation of the respective carbonized fibers is shown in Figures 3 and 4. Ridges are apparent on the surfaces of the petroleum fibers, and they tend to follow the fiber circumference. Despite this, the surface appears relatively smooth and there are no evident cracks or pores. With the shale oil fibers, an irregular distribution of small pits or pores have developed over the fiber surfaces. In addition, particles can be observed on the surfaces of some of the pore walls. It may be that some of the ash components can have a catalytic influence on the activation or gasification of the fibers, and are instrumental in the generation of these features. The SEM micrographs also suggest that there are some differences in the internal morphology of the two types of fiber.

As shown in Table 3, under similar conditions, the shale oil carbon fibers experienced much greater burn-off during steam activation than the petroleum pitch fibers. This finding also indicates that the former are more reactive to reactions with oxidizing gases, either due to certain inherent aspects of their composition and structure, or to the catalytic effect of ash constituents. Predictably, activation in carbon dioxide, which is known to be a slower reaction, caused lower burn-off than steam under the same conditions. Despite the different degrees of burn-off, the steam activated fibers from pitch and shale oil had very similar BET surface areas. There may be significant differences in their pore size distributions, although this has yet to be determined, as does the dependence of pore structure on burn off.

### ***Nitrogen Content***

The changes in nitrogen content (N/C atomic ratio) during carbonization and activation for both kinds of precursor are shown in Figure 5. For the petroleum pitch, the nitrogen content increased upon carbonization and then kept unchanged through steam activation. As already noted, the N/C atomic ratio was much higher in the shale oil asphaltenes. It was slightly reduced upon carbonization, and then remained at a similar level upon activation: the N/C ratio for activated carbon fibers was about 0.025.

### ***Synopsis***

Preliminary studies have been made of the feasibility of producing carbon fibers from high boiling shale oil liquids. Single filament carbon fibers and activated carbon fibers have been produced successfully from an asphaltene fraction of shale oil residuum, by spinning, oxidative stabilization, carbonization, and activation. Comparisons were made with fibers derived from a petroleum pitch.

The yield of the shale oil carbonized fibers was around 50% while that for the petroleum pitch was about 70%. Differences in yield are attributed to the different volatile contents of the precursors.

Activated carbon fibers were obtained by steam activation of the carbonized fibers at 850°C. A BET surface area of around 960 m<sup>2</sup>/g was obtained at 63% burn off for the shale oil fibers. A similar surface area was obtained for the petroleum pitch based fiber after reaction under the same conditions but with only 38% burn off. The greater reactivity of the shale oil fibers may be due to

their inherent structure and/or to the catalytic effect of ash constituents: some evidence for catalysis is provided by microscopic observations. High reactivity of green fibers is also indicated by the low reaction temperature required for oxidative stabilization. The high nitrogen content of the activated shale oil fibers may provide unusual adsorptive or catalytic properties.

### Acknowledgments

The authors wish to thank Mark Stewart and Darrell Taulbee of the University of Kentucky Center for Applied Energy Research for surface area measurements, and for providing shale oil liquids, respectively.

### References

1. S.A. Homes and L.F. Thompson, Proc. 14th Oil Shale Symposium, Colorado, 1981, p.235.
2. J.W. Bunker, P.A.V. Devineni and D.E. Cogswell, American Chemical Society, Fuel Division Reprint, 37(2), 581(1992).
3. G.P. Daumit, Carbon, 27(5), 759(1989).
4. L.S. Singer, in Concise Encyclopedia of Composite Materials, Edited by Anthony Kelly, The MIT Press, 1989, p.47.
5. I.N.Ermolenko, I.P.Lyubliner and N.V.Gulko, in Chemically Modified Carbon Fibers, (Translated by E.P.Titovets), VCH Publisher, New York, 1990, p.198.
6. H. Fujitsu and I. Mochida, in Kaseitan (Activated Carbon), Edited by Y. Sanada, M. Suzuki and K. Fujimoto, Kotansha Scientific, Tokyo, 1992, p.195.
7. K. Sato, M. Hirai and K. Shimazaki, TEXTILE TEKHNOLGY'84, Industrial Fabrics Association International 72nd Annual Convention, 1984.
8. I. Mochida, Y.N. Sun, H. Fujitsu, S. Kisamori and S. Kawano, Nippon Kagakugakaishi (J.Chemical Society of Japan) No.6, 885 (1991).
9. S.D. Carter, T. Robl, A.M. Rubel and D.N. Taulbee, Fuel, 69(9), 1124 (1990).
10. Y.Q. Fei, K. Sakanishi, Y.N. Sun, R. Yamashita and I. Mochida, Fuel, 69(2), 261 (1990).
11. J.B. Donnet and R.C. Bansal, in Carbon Fiber, Marcel Dekker, New York, 1990, p.55.

Table 1 Analyses of precursor materials

Sample *	Elemental Analysis (wt%)				Atomic Ratio (%)		Content of Ash (wt%)	Softening Point (°C)
	C	H	N	S	H/C	N/C		
PP	92.88	4.63	0.31	1.99	0.60	0.29	0.21	258
SOR	83.22	9.60	0.51	1.82	1.38	0.53	0.82	< 25
SOR-AS	80.98	6.64	2.54	1.96	0.98	2.69	0.97	183

\* PP, petroleum-derived isotropic pitch; SOR, shale oil residue; SOR-AS, asphaltenes: hexane insoluble, benzene soluble.

**Table 2 Carbonization of two kinds of green fibers**

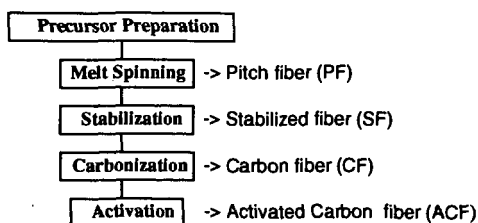
Sample Code	Precursor Type	Yield (wt%)*	Diameter of CF (mm)
CF-P1	PP	71	6 ~ 15
CF-S1	SOR-AS	50	5 ~ 12

\* carbonized at 850°C for 30 min; yield as % of green fibers.

**Table 3 Activation of petroleum and shale oil-derived carbon fibers**

Sample Code	Precursor Type	Activating Agents	Burn-off (wt%)*	Diameter of ACF (mm)	Surface Area (m <sup>2</sup> /g)
AF-P1	PP	H <sub>2</sub> O/N <sub>2</sub> (50:50)	38	4 ~ 12	978
AF-S1	SOR-AS	H <sub>2</sub> O/N <sub>2</sub> (50:50)	63	3 ~ 10	960
AF-S2	SOR-AS	CO <sub>2</sub> /N <sub>2</sub> (50:50)	49	3 ~ 10	566

\* activation at 850°C for 60 min; yield as % of carbonized fibers.

**Figure 1** Flowsheet of the preparation of carbon fibers and activated carbon fibers.

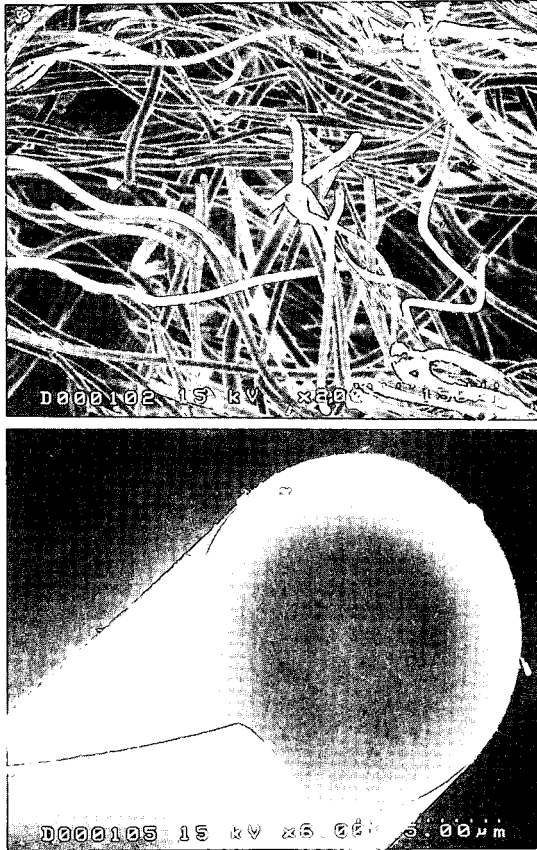


Figure 2 SEM micrographs of carbon fibers produced from shale oil.

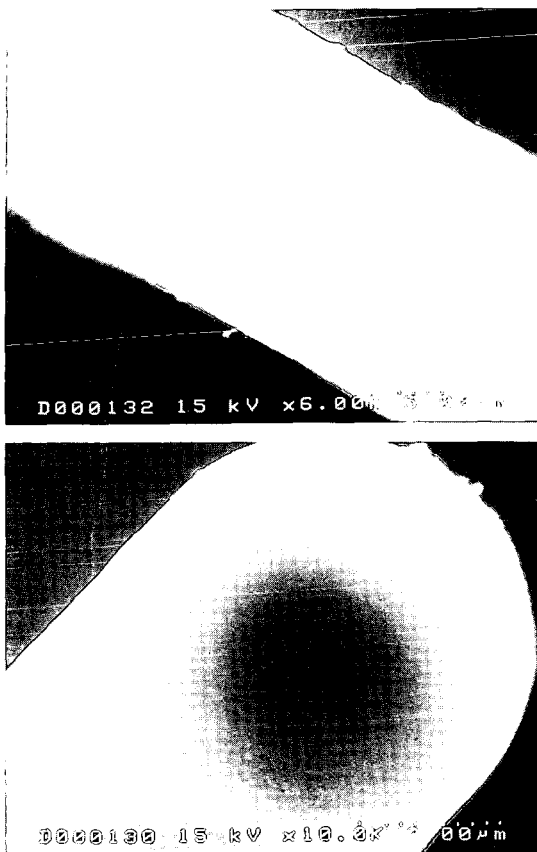


Figure 3 SEM micrographs of activated carbon fibers from petroleum pitch by steam activation.

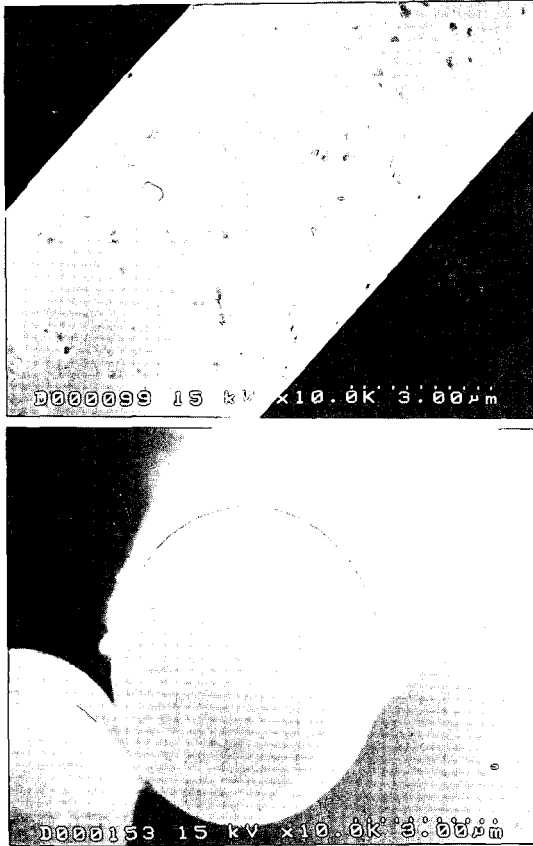


Figure 4 SEM micrographs of activated carbon fibers from shale oil by steam activation.

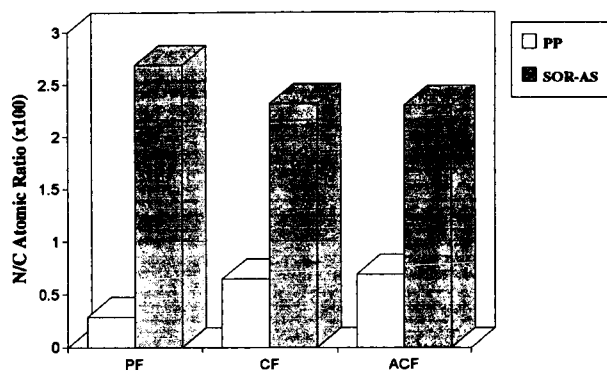


Figure 5 Changes in nitrogen content during the preparation of carbon fibers and activated carbon fibers from shale oil (SOR-AS) and petroleum (PP) precursors.

## HIGH PERFORMANCE, MODERATE COST MESOPHASE PITCH BASED CARBON FIBERS

I. Mochida, Y. Korai, S. H. Yoon, F. Fortin, L. C. Ling, K. Kanno\*

Institute of Advanced Material Study, Kyushu University,  
Kasuga, Fukuoka 816, Japan

\*Mitsubishi Gas Chemical Company, Inc.  
Chiyoda-ku Tokyo 100, Japan

### ABSTRACT

Mesophase pitch has been successfully prepared at very highly yield from aromatic hydrocarbons with low contaminant levels using HF/BF<sub>3</sub> as the catalyst. The derived carbon fiber is expected to be of high performance and to be produced at reasonable cost. The synthesis, structure, and properties of the mesophase pitches, which are strongly dependent upon the starting aromatic hydrocarbons and preparation conditions, will be described. The spinning process can control the shape and texture of the fiber, both of which are intimately related to performance. Fibers with a flat cross section, as thin as 1.5 μm, and round fibers with random texture can be produced when the spinning nozzle and the mesophase pitch are properly selected. Acceptable compression strength has been obtained with the random texture in the round fiber. Very high tensile strength as well as Young's modulus are realized by slow heating during stabilization. Some other applications of mesophase pitch will be addressed.

Key words: Mesophase pitch, Carbon fiber, HF/BF<sub>3</sub>

### INTRODUCTION

Mesophase pitch has been recognized as the most promising precursor for the carbon fiber of excellent properties and reasonable cost. Because of their low price, the residues from coal tar as well as petroleum have been selected as the starting substances. However, high cost of their refining, the lower yield, difficulty in spinning or the control of their molecular structure, and low reactivity lead to unacceptable price and insufficient quality. Carbon fibers produced from latter ones are of high price and their properties are unsatisfactory except for better Young's modulus which is better than that of PAN-based one<sup>1)-3)</sup>, limiting the broad application. Hence, lower price and better performances of the mesophase pitch are most relevant for the pitch based high performance carbon fiber.

Mitsubishi Gas Chemical company and Kyushu University proposed an application of HF/BF<sub>3</sub> as the catalyst for the condensation of aromatic hydrocarbon into mesophase pitch<sup>4)-11)</sup>. In the present paper, preparation conditions, structure, and physical and chemical properties of the mesophase pitch produced using HF/BF<sub>3</sub> were examined.

## EXPERIMENTAL

HF and  $\text{BF}_3$  are low boiling points of 19.9 and  $-101.1^\circ\text{C}$ , respectively. Such a liquid and a gas catalysts can promote the homogeneous reaction of monomer, being recovered and recycled completely by the distillation. HF has high dissolving power for organic compounds and can accelerate ionic reaction through the carbenium ion because of its high polarity. The ionic polymerization at lower temperatures is able to design the structure of mesophase pitch by virtue of the selective reaction under mild preparative conditions. Thus, mesophase pitches from naphthalene, anthracene and methylnaphthalene were prepared directly using HF/ $\text{BF}_3$  at a temperature range of 180 -  $300^\circ\text{C}$ .

These mesophase pitches were spun into fiber using mono hole spinneret of round, Y and slit shape under various conditions. After stabilization in air, fibers are carbonized in argon at 1300 to  $2500^\circ\text{C}$ .

## RESULTS AND DISCUSSION

### 1. Preparation of mesophase pitch

Catalytic polymerization reactions of naphthalene are illustrated in Fig. 1. The protonated complex exists in excess HF as a suitable proton donor. It reacts with other monomer at the position of the highest electron density to produce dimeric structure without dehydrogenation. Such a non-dehydrogenative reaction will be repeated to produce aromatic oligomers such as trimers and tetramers, carrying hydrogens as many as a number of polymerization reaction. These hydrogens are finally stabilized in the produced pitch as naphthenic hydrogens.

Preparation conditions of pitches at a temperature range of 180 to  $300^\circ\text{C}$  are shown in Table 1. Mesophase pitch of 100 vol% anisotropy could be prepared catalytically from naphthalene at  $210 - 300^\circ\text{C}$ . Amount of HF and  $\text{BF}_3$  is important to develop the anisotropy, no anisotropy being observed when ratios of HF/naphthalene and  $\text{BF}_3$ /naphthalene were 0.30 and 0.15 in molar ratio at  $260^\circ\text{C}$ , respectively. However, a higher temperature ( $300^\circ\text{C}$ ) induced 100 vol% anisotropy even with a small amount of HF/ $\text{BF}_3$ . Mesophase pitch of 100 vol% anisotropy could be prepared directly from anthracene at  $220^\circ\text{C}$ . Anthracene is more reactive than naphthalene, providing the pitch of higher softening point with a small amount of the catalyst. The larger planar of anthracene may be favorable for its oligomer to develop anisotropy. Mesophase pitch of 100 vol% anisotropy could be prepared also from methylnaphthalene at  $265^\circ\text{C}$  for 5 h under autogenous pressure in an autoclave. Its softening point of  $205^\circ\text{C}$  should be noted very low, suggesting that methyl group of the monomer influences on properties of the resultant mesophase pitch. A pitch prepared from methylnaphthalene at  $260^\circ\text{C}$  by the same period carried 80 vol% of anisotropy. The methyl group may hinder cationic polymerization.

### 2. Some properties of mesophase pitches

General properties of mesophase pitches prepared from naphthalene, anthracene, methylnaphthalene are summarized in Table 2. Their softening point, solubility, H/C

ratio varied according to preparation temperature and starting materials. Anthracene mesophase pitch tends to exhibit higher softening point and a low solubility. Methyl naphthalene pitch has a softening point of as low as 205°C and 57 % solubility in benzene.

**Table 3** summarizes the hydrogen distribution in the BS and BI-PS fractions of the mesophase pitches. The higher preparation temperature tends to provide a more aromatic mesophase pitch. Aromaticity of anthracene mesophase pitch (AP-220) and naphthalene mesophase pitch (NP-260) are similar. The methyl naphthalene mesophase pitch is most aliphatic, carrying many methyl groups in spite of the severest preparation conditions. The representative molecular species of BS fraction of each mesophase pitches are illustrated in **Fig. 2**.

### **3. Molecular assembly of the mesophase pitches**

Molecular assembly of the mesophase pitches at their fused states is examined using a high temperature horizontal X-ray diffractometer<sup>12)</sup>. Changes in Lc values of some pitches calculated from the half width of C(002) are shown in **Fig. 3**. MNP-265 shows the largest Lc value of 5.8 nm at room temperature which stays almost constant up to 210°C of its softening point. Then, Lc decreases sharply at higher temperatures than its softening point. At 350°C, Lc of MNP-265 decreases to less than a half of that at room temperature. These results reveal that the mesogen molecules in the mesophase pitch are certainly stacked as observed with conventional liquid crystals, the thickness or number and d-space of the layers being temperature-dependent and different from one pitch to another. Among the mesophase pitch, MNP-265, exhibits the largest Lc (average thickness).

The values of Lc change according to the temperature especially above the softening point. The thermal motion of molecules above the softening point may compete the intermolecular interaction to liberate the stacking and to enlarge the d-space. Lc in MNP-265 decreases most sharply and those of NP-265-5 and AP-220 do gradually. The molecular motion should influence the stacking thickness and d-space in the similar manners, however, the former should be also influenced by the solubility of the stacking fraction in the isotropic matrix which is more strongly molecular structure - dependent.

### **4. Viscoelastic properties of mesophase pitches**

The mesophase pitch exhibited viscoelastic properties, reflecting its molecular structure and assembly. Typical viscoelastic properties of MNP-265 and NP-265-5 are shown in **Fig. 4**. Very different profiles may be due to the different assembling structure described above. The viscoelastic properties define the alignment in the spinning nozzle, dieswelling at the outlet of nozzle, and alignment at the extension. Hence such properties influence strength, shape, and texture of the resultant carbon fiber.

### **5. Carbon fiber from the mesophase pitch**

A variety of mesophase pitches provide various pitch based carbon fibers, which can achieve high tensile strength, Young's modulus<sup>1),2)</sup> and compressive strength. Shapes of molecules and their stacking influence alignment of aromatic planes in

the pitch fiber under the spinning conditions which are fixed by stabilization. The alignment, thickness, and length of the graphite units along the fiber axis are recognized as the common origin of these strengths, the thicker the stacking the higher the modulus or stiffness of the carbon fiber. This occurs at a sacrifice of compressive strength. Hence, the complete controls of molecular shape and its alignment during the preparation of mesophase pitch and spinning are major targets to be achieved for the development of higher performance pitch-based carbon fiber. Table 4 summarizes the mechanical properties of carbonized fibers from naphthalene(NP-260-3) and anthracene(AP-220) mesophase pitches. Tensile strength of their carbonized fiber from NP-260-3 was 2.60 GPa at 1500°C and gradually increased with graphitization, reaching higher than 3.0 GPa by 2550°C. In contrast, tensile strength of carbonized fiber from AP-220 was limited to around 2.0 GPa, even after graphitization at 2550°C, indicating defects at its spinning. Tensile modulus of both fibers are very high, achieving 800 GPa by 2550°C. AP-220 tends to give higher values of Young's modulus than NP-260-3 when the graphitization temperature is lower. It may be due to the constituent molecules of the former mesophase pitch which consist of anthracene units tend to have wider planar structure for developing better graphitization and orientation. Because the spinning properties of AP-220 is inferior to that of NP-260-3, tensile strength of the former fibers may be limited due to micro-defects introduced at spinning. Careful preparation of AP-220 for its better spinning is expected to increase the tensile strength of its resultant carbon fiber.

#### **6. Improvement of mechanical properties of pitch based carbon fiber**

Because the physical properties and mechanical properties of carbon fibers strongly depend on their transversal shape and texture<sup>(3)-15)</sup>, it is believed that controls of transversal shape and texture of carbon fiber during the spinning is most relevant<sup>14)</sup>. The present authors examined some methods to change the flow pattern of molten pitches during spinning in order to control the transversal texture. Fig. 5 shows transversal sections of carbon fibers from methylnaphthalene derived mesophase pitch (MNP-265), using circular or non-circular shaped spinning nozzles at 285°C. It is noted that circular shaped fiber is obtainable at this temperature regardless of the nozzle shapes. Transversal texture of carbon fibers from Y and slit shaped spinning nozzles exhibited random or random-onion textures, respectively. In contrast, circular shaped spinning nozzle gives a radial one with open wedge, even though melt viscosities of molten pitches are much the same at the spinning temperature. This indicates that the flow pattern of molten mesophase pitch is changed and distorted against fiber axis during extrusion before solidification.

Table 5 shows mechanical properties of carbon fibers. Tensile strengths of graphitized carbon fibers spun with Y and slit shaped spinning nozzles are improved by 0.25 and 0.55 GPa, respectively. Young's modulus and compressive strengths of graphitized fibers spun with Y and slit shaped spinning nozzles are also improved by 160 and 0.13 GPa, and 120 and 0.04 GPa, respectively. Importance to control the texture is suggested to improve the mechanical properties of the resultant fiber. Slow heating rate of 0.5°C at the stabilization was found to improve very significantly the tensile strength up to 5 GPa.

Fig. 6 shows the transversal shape and texture of graphitized tape, which is spun through the slit nozzle. The thickness of the tape is as thin as  $1.6\ \mu\text{m}^{15}$ . Its excellent mechanical properties are noted. Tensile strength, Young's modulus and compressive strength of the graphitized tape are as high as 3.65 GPa, 810 GPa, and 0.71 GPa, respectively.

### 7. Further application of the mesophase pitch

The present mesophase pitches with moderate softening points and naphthenic hydrogens can be used as precursor pitches for a variety of carbon materials. The following are some examples: Carbon fiber-mesophase pitch prepreg<sup>17</sup>, high density carbon materials, binder of MgO brick<sup>18</sup>, porous carbonaceous materials, precursor for the solid lubricant, and oxidation prohibitors.

### REFERENCES

- 1) S. Ohtani, A. Watanabe and H. Ogino, Bull. Chem. Soc. Japan **45**, 3715 (1972)
- 2) L. S. Singer, Fuel **60**, 839 (1981)
- 3) E. Fitzer, Carbon **27**, 62(1989)
- 4) I. Mochida, K. Shimizu, Y. Korai, H. Otsuka and S. Fujiyama, Carbon **26**, 843 (1988)
- 5) I. Mochida, K. Shimizu, Y. Korai, Y. Sakai and S. Fujiyama, Chem. Lett. 1893 (1989)
- 6) I. Mochida, K. Shimizu, Y. Korai, H. Otsuka, Y. Sakai and S. Fujiyama, Carbon **28**, 311 (1990)
- 7) I. Mochida, K. Shimizu, Y. Korai, Y. Sakai and S. Fujiyama, Bull. Chem. Soc. Japan **63**, 2945 (1990)
- 8) I. Mochida, K. Shimizu, Y. Korai, Y. Sakai, S. Fujiyama, H. Toshima and T. Hino, Carbon **30**, 55 (1992)
- 9) I. Mochida, K. Shimizu, Y. Korai, Y. Sakai and S. Fujiyama, High Temperature-High Pressure, in press.
- 10) I. Mochida and S. Fujiyama, Japanese Open Patent Shouwa 63-146920 (1988)
- 11) I. Mochida, Y. Sakai and H. Ohtsuka, Japanese Open Patent Heisei 1-139621(1989)
- 12) Y. Korai and I. Mochida, Carbon **30**, 1019 (1992)
- 13) I. Mochida, S. H. Yoon, and Y. Korai, J. Mater. Sci. to be published
- 14) I. Mochida, S. H. Yoon, and Y. Korai, J. Mater. Sci. in press
- 15) I. Mochida, S. H. Yoon, and Y. Korai, Chem. Letter. 1111 (1992)
- 16) H. M. Hawthorne and E. Teghtsoonian, J. Mater. Sci. **22**, 41 (1975)
- 17) I. Mochida, R. Fujiura and Y. Korai, TANSO, No.155, p.398 (1992)
- 18) I. Mochida, Y. Korai, N. Akashi, R. Fujiura and K. Ito, TANSO No.149, p.256 (1991)

Table 1 Preparation conditions of pitches and their some properties.

Sample	HF (mol%)	BF <sub>3</sub> (mol%)	Temp. (°C)	Yield (wt%)	A. C. (vol%)	S. P. (°C)
NP-180	0.67	0.25	180	52	0	202
NP-200	0.81	0.30	200	52	15	199
NP-210	0.83	0.30	210	74	98	216
NP-260-1	0.59	0.15	260	71	95	219
NP-260-2	0.30	0.25	260	37	0	95
NP-260-3	0.47	0.20	260	68	100	212
NP-300	0.64	0.10	300	58	100	285
AP-220	1.00	0.20	220	90	100	238
AP-260	1.00	0.10	260	82	100	275
MNP-260	0.52	0.15	260	>80	80	205
MNP-265	0.52	0.15	265	76	100	205

NP: naphthalene derived pitch., AP: anthracene derived pitch.

MNP: methylnaphthalene derived pitch.

The amount of aromatic hydrocarbon: 1 mol.

Preparation time is 4 hr except for MNP-265(5 hr)

Table 2 Some properties of mesophase pitches.

Sample	S.P. (°C)	A. C. (vol%)	Solubility(wt%)				H/C
			BS	BI-PS	PI-QS	QI	
NP-260-4	215	100	52	19	6	23	0.67
NP-260-5	212	100	57	15	12	16	-
NP-300	285	100	12	29	6	53	0.58
AP-220	238	100	44	12	19	25	0.62
AP-260	275	100	19	32	16	33	0.65
MNP-260	205	80	72	10	10	8	0.68
MNP-265	205	100	57	13	4	26	0.69

Table 3 Hydrogen distribution of BS and BI-PS fractions in the mesophase pitches.

		Hydrogen distribution(%)				
		Haro	H <sub>α</sub>	H <sub>β</sub>	H <sub>γ</sub>	fa
NP-260-4	BS	50	36	13	1	0.82
	BI-PS	66	25	8	1	0.90
NP-300	BS	65	23	10	2	0.89
	BI-PS	71	15	9	5	0.92
AP-220	BS	56	26	15	3	0.85
	BI-PS	57	20	19	4	0.87
MNP-265	BS	44	40	13	3	0.81
	BI-PS	47	35	15	3	-

Haro: aromatic hydrogen(6-10 ppm), H<sub>α</sub>: α-position hydrogen(2.1-5.0 ppm)

H<sub>β</sub>: β-position hydrogen(1.1-2.1 ppm), H<sub>γ</sub>: γ-position hydrogen(0.3-1.1 ppm)

fa: aromaticity

Table 4 Mechanical properties of carbon fiber produced from NP and AP.

	HTT (°C)	$\Delta l$ (%)	T.S. <sup>1)</sup> (GPa)	Y.M. <sup>1)</sup> (GPa)
NP-260-3	1500	1.0	2.60	250
	2000	0.6	2.50	500
	2550	0.4	3.50	800
AP-220	1500	0.6	1.70	270
	2000	0.3	2.00	570
	2550	0.3	2.00	810

1) JIS R7601 monofilament method

HTT: heat-treatment temperature,

T.S.: tensile strength,

$\Delta l$ : strain to break,

Y.M.: Young's modulus

Table 5 Mechanical properties of graphitized fibers.

nozzle	fiber. shape	texture	diameter ( $\mu\text{m}$ )	$\Delta l$ (%)	DO (%)	Lc (nm)	T.S. (GPa)	Y.M. (GPa)	CS (GPa)
circular	circular	radial-crack	7.0	0.35	95.4	21	2.85	740	0.58
Y	triangle	random	9.0	0.40	94.2	39	3.10	900	0.71
slit	circular	random-onion	9.0	0.45	95.4	23	3.40	860	0.62

DO: degree of orientation

CS: compressive strength tested by composit method( $V_f=60\%$ )  
proposed by H. M. Hawthorne et. al. (ref. 15)

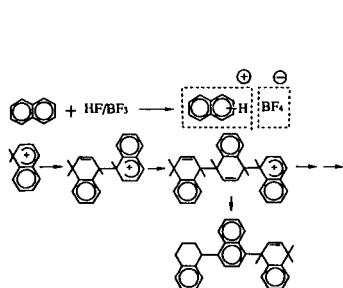


Fig. 1 Catalytic polymerization of naphthalene with  $\text{HF}/\text{BF}_3$ .

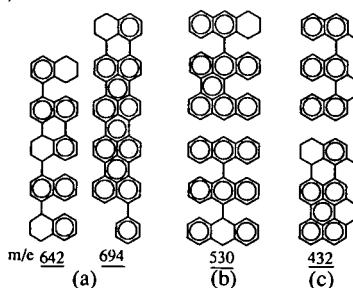


Fig. 2 Model structure of BS in the mesophase pitches.  
(a)NP-260, (b)AP-220, (c)MNP-265

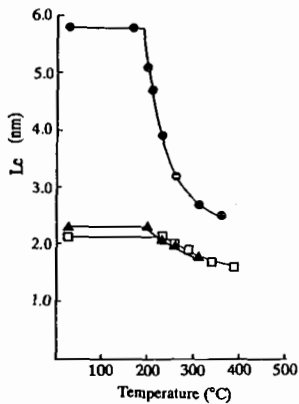


Fig. 3 Change in  $L_c$  at higher temperatures.  
 ○:MNP-265, ▲:NP-265-5,  
 □:AP-220

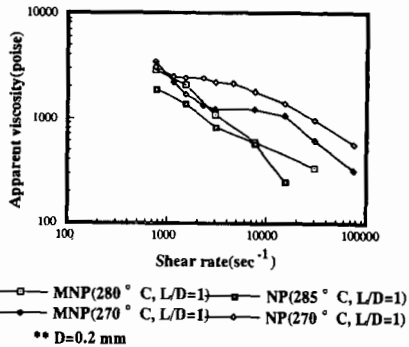


Fig. 4 Typical viscoelastic properties of MNP-265 and NP-265-5

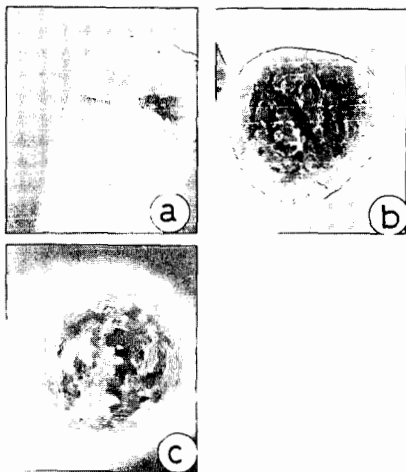


Fig. 5 SEM photographs of carbon fibers spun with circular or non-circular shaped spinning nozzles.  
 (a) circular-shaped nozzle  
 (b) Y-shaped nozzle  
 (c) slit-shaped nozzle

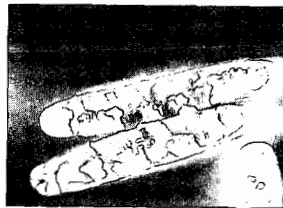


Fig. 6 SEM photograph of carbon tape graphitized at 2500°C

## LASER PYROLYSIS PRODUCTION OF NANOSCALE CARBON BLACK

Xiang-Xin Bi<sup>1</sup>, Wen-tse Lee<sup>1</sup> and Peter C. Eklund<sup>1,2</sup>

<sup>1</sup>Center for Applied Energy Research

<sup>2</sup>Department of Physics and Astronomy

University of Kentucky

Lexington, KY40506, USA

M. Endo<sup>3</sup>, K. Takeuchi<sup>3</sup>, S. Igarashi<sup>3</sup>, and M. Shiraishi<sup>4</sup>

<sup>3</sup>Shinshu University

Department of Electrical Engineering

<sup>4</sup>National Research Institute for Resources and Environment

Nagano-city 380, JAPAN

Key words: laser pyrolysis, carbon black, catalysis, fullerenes

### INTRODUCTION

Laser pyrolysis [1] is a versatile non-equilibrium thermodynamic process for the production of nanoscale particles involving fast growth, and rapid heating/cooling rates (~100,000 °C/s) in the reaction zone defined by the intersection of a reactant gas stream and high power infrared (CO<sub>2</sub>) laser. Using this technique, we have recently produced nearly pure phase nanocrystalline particles of  $\alpha$ -Fe, Fe<sub>3</sub>C, and Fe<sub>7</sub>C<sub>3</sub> [2]. This research, and our interest in fullerenes (e.g., C<sub>60</sub>), motivated us to consider whether or not we could extend the laser pyrolysis technique to produce the other endpoint material, e.g., pure, or nearly pure nanocrystalline carbon, and perhaps fullerenes. CO<sub>2</sub> laser pyrolysis production of carbon soot from acetylene (C<sub>2</sub>H<sub>2</sub>) decomposition was reported by Maleissye et al. [3] and Yampolskii et al. [4]. They found reaction products are close to those obtained in a classic pyrolysis. In this paper, we report the results of a study involving catalytic decomposition of benzene (C<sub>6</sub>H<sub>6</sub>) to produce carbon black. Using small quantities of Fe as a catalyst, we obtained nearly pure carbon soot comprised of amorphous, spherical carbon particles with an average dia.~ 20 nm. These carbon nanoparticles appear to best resemble acetylene black, which identifies a nanoscale carbon soot prepared by the oxidation or thermal decomposition of acetylene [5]. We have furthermore subjected our nanoscale soot to a 2800 °C high temperature treatment (HTT) under Ar gas which promotes the transformation of the disordered spherical soot particles to particles of approximately the same size, but with polygonal facets and, in many cases, a hollow core. Pyrolytic carbon planes are observed aligned parallel to the facets on the heat treated particles, as seen in TEM lattice fringe images. We have no evidence, as yet, that fullerenes were produced along with the nanoscale soot.

To produce nanocrystalline  $\alpha$ -Fe and Fe-carbides, we have investigated recently the laser driven reaction of Fe(CO)<sub>5</sub> and ethylene (C<sub>2</sub>H<sub>4</sub>) following the process described in patents submitted by Exxon researchers [6, 7] who reported the production of Fe<sub>3</sub>C (cementite). To produce carbon black as an extension of this reaction, we first tried the obvious step, namely that of reducing the relative concentration of Fe(CO)<sub>5</sub> in the reactant gas stream. These experiments failed to produce significant amounts of carbon black, yielding instead nanoscale Fe<sub>7</sub>C<sub>3</sub> with a thick coating of pyrolytic carbon. We next tried the addition of benzene (C<sub>6</sub>H<sub>6</sub>) to the reactant gas stream, and large amounts of fairly uniform size nanoscale carbon soot was thereby produced. Subsequent experiments revealed that this reaction requires the presence of only small amounts of

Fe(as a catalyst) to promote the formation of the carbon black. Carbon soot prepared in this way is the subject of this paper.

## SYNTHESIS

Our laser pyrolysis system is shown schematically in Fig. 1, and is similar to that described by Haggerty [1]. The reactants ( $\text{Fe}(\text{CO})_5$ ,  $\text{C}_2\text{H}_4$  (99.99%) and  $\text{C}_6\text{H}_6$  (HPLC grade)) are introduced into the reactant gas stream by bubbling  $\text{C}_2\text{H}_4$  through a solution of  $\text{C}_6\text{H}_6:\text{Fe}(\text{CO})_5 = 50:1$  (by volume) contained in a trap, as shown. The reactant gases then flow vertically out of a stainless steel nozzle inside the 6-way stainless steel cross (chamber) and intersect a horizontal beam from a  $\text{CO}_2$  laser (Laser Photonics Model 150). The  $\text{C}_2\text{H}_4$  flow rate was regulated to be  $\sim 100$  sccm. Using  $\sim 15,000\text{W}/\text{mm}^2$  incident power density in the reaction zone, a bright white flame was observed. The energy coupling of the laser to the reactant gas is realized by tuning the laser frequency to the P20 line ( $945\text{ cm}^{-1}$ ), which is shifted  $5\text{ cm}^{-1}$  relative to the strongest nearby rotational-vibrational absorption line of  $\text{C}_2\text{H}_4$  at  $950\text{ cm}^{-1}$ . A ZnSe lens was used to adjust the position of the  $\text{CO}_2$  laser beam waist relative to the nozzle tip. If no  $\text{Fe}(\text{CO})_5$  is present in the stream, almost no soot is produced. From our previous work [2], if no benzene is present (only  $\text{C}_2\text{H}_4$  and  $\text{Fe}(\text{CO})_5$ ), then Fe-carbides are formed. We therefore speculate that  $\text{Fe}(\text{CO})_5$  in the presence of both  $\text{C}_2\text{H}_4$  and  $\text{C}_6\text{H}_6$  acts as a catalyst, dehydrogenating the benzene and forcing the benzene molecule to fragment in the pyrolysis flame, leading to carbon soot formation. The chemical role of the  $\text{C}_2\text{H}_4$  may not be important, other than to allow heat energy from the laser to be pumped into the reaction.

After leaving the pyrolysis zone, the particles, protected by a lamellar, co-axial flow of Ar gas, are collected in a Pyrex trap (Fig. 1). A teflon membrane filter (pore size 200 nm) was used to protect the mechanical pump. In the steady state, using a reactant gas nozzle with circular 5 mm dia. opening, a 4 - 6 mm diameter, well-collimated stream of particles can be seen to drift up the center of the 1 cm (I.D.) glass tube connecting the 6-way cross and Pyrex particle trap. A 0.5g/hour production rate of carbon black was obtained under the conditions described above. Mass flow controllers were used to control the supply of Ar (99.999%) to the coaxial sheath and to the cell windows; a separate controller was used to control the flow of the reactant gas mixture. Further details of our laser pyrolysis apparatus are available elsewhere [2].

## RESULTS AND DISCUSSION

Subsequent to the synthesis, standard elemental analyses were applied to our carbon black samples for Fe, C, N, and H. The results of this analysis yield a composition  $\text{C}_{10}\text{Fe}_{0.01}\text{H}_{1.2}\text{N}_{0.1}$ . It should be noted that the C:H ratio is  $\sim 8$ , close to the ideal value  $\sim 10$  predicted for acetylene black using a polycondensation model, and this value is lower than that obtained for a typical acetylene black, which has C:H  $\sim 40$  [5]. The C:Fe ratio was also measured using electron microprobe analysis (EDX), resulting in C:Fe  $\sim 700$ , consistent with the value  $\sim 1000$  obtained from the elemental analysis.

Shown in Fig. 2 are the high resolution TEM data taken using a JOEL 4000 electron microscope on "as synthesized" (2a, 2b) and heat treated ( $2800^\circ\text{C}$  in Ar) (2c, 2d) carbon blacks produced by laser pyrolysis. As shown in Fig. 2a, untreated carbon black particles present, on average, a well developed spherical shape, with an average particle diameter on the order

of 20 nm. Typical of acetylene black, significant agglomeration was observed [5]. It is difficult to determine to what extent the particles might be fused, however. Fig. 2b is a magnified image within particle. Although the formation of very primitive carbon planes is observable in some regions of selected particles, most carbon black particles appear to exhibit an image of a highly disordered graphitic carbon (see the discussion of the x-ray results below).

Using the standard N<sub>2</sub> BET technique, we determined a value 50 m<sup>2</sup>/g surface area for the "as-synthesized" carbon black. This value is slightly lower than 70 m<sup>2</sup>/g reported for a typical acetylene black, and is lower than the theoretical surface total surface area for a 20 nm spherical particles (150 m<sup>2</sup>/g). Consistent with this observation of a lower surface area, is that no significant cracking of the particle surface or accessible internal pores are apparent in the TEM photos (Fig. 2b) and that agglomeration (with possible fusion) of the particles is also observed.

Furthermore, the carbon black samples subjected to 2800 °C HTT in Ar show clear evidence for graphitization, consistent with lattice fringes from parallel carbon planes and the associated lattice plane spacing (Fig. 2d). As shown in Fig. 2c and 2d, heat treated particles, in many cases, exhibit parallel carbon layers in polygonal shapes about a hollow center. This suggests that crystallization is initiated at the particle surface. Finally, we did not observe any evidence for the presence of Fe or Fe carbides as small particles within the carbon black particle, or, in particular, at the particle core, or as a separate nanoparticle. This is consistent with the small amount of Fe observed in the carbon black (0.5wt %), suggesting that the Fe may be atomically dispersed throughout the soot.

Shown in Fig. 3 are XRD results obtained with a Rigaku powder diffraction unit using Cu K<sub>α</sub> radiation. Results for "as synthesized" (Fig. 3a) and low temperature HTT (900 °C in N<sub>2</sub>) (Fig. 3b) carbon black samples are presented. The low HTT sample was produced with a higher than normal amount of Fe(CO)<sub>5</sub>. As a result, this sample exhibited x-ray diffraction peaks associated with the existence of nanocrystalline α-Fe and γ-Fe, as indicated. The diffraction peaks for the "as synthesized" sample are similar in width to that of a typical acetylene black [5]. Broad peaks are observed and indexed according to a convention for acetylene blacks based on graphite: in decreasing intensity, they are the 002, 10, and 11 diffraction lines, respectively. The average lattice constant along the c-axis, as determined from the 002 peak position, is found to be 3.65 Å, somewhat larger than normally observed (<3.5 Å) for acetylene black. A significant shift of 002 peak is observed after a 900 °C HTT in N<sub>2</sub> for 24 hrs (Fig. 3b), where again from the 002 peak, the lattice constant has decreased to 3.48 Å, closer to that of a typical acetylene black (3.43 Å).

Further work will be necessary to determine the role of Fe as a catalyst in the production of carbon black by the laser pyrolysis process.

#### ACKNOWLEDGEMENTS

This work was supported, in part, by the University of Kentucky Center for Applied Energy Research and the United States Department of Energy. We wish to thank Gerald Thomas and Mark Stewart for assistance in the characterization of the carbon black, and acknowledge helpful discussions with Frank Derbyshire.

## REFERENCES

1. J. S. Haggerty, "Sinterable Powders from Laser-Driven Reactions", in *Laser-induced Chemical Processes*, Editor, J.I. Steinfeld, 1981, Plenum Press: New York.
2. Xiang-Xin Bi, B. Ganguly, G. Huffman, E. Huggines, M. Endo, and P. C. Eklund, *J. of Material Research*, Submitted, 1992.
3. J. T. d. Maleissye, F. Lempereur, and C. Marsal, *C. R. Acad. Sci., Paris, Ser.*, **275**: p. 1153, 1972.
4. Y. P. Yampolskii, Y. V. Maximov, N. P. Novikov, and K. P. Lavrovskii, *Khim. Vys. Energ.*, **4**: p. 283, 1970.
5. Y. Schwob, "Acetylene Black: Manufacture, Properties, and Applications", in *Chemistry and Physics of Carbon*, Editor, J. Philip L. Walker and P.A. Thrower, 1979, Marcel Dekker, Inc.: New York and Basel. p. 109.
6. R. A. Fiato, G. W. Rice, S. Miso, and S. L. Soled, United States Patent, **4,637,753**1987.
7. G. W. Rice, R. A. Fiato, and S. L. Soled, United States Patent, **4,659,681**1987.

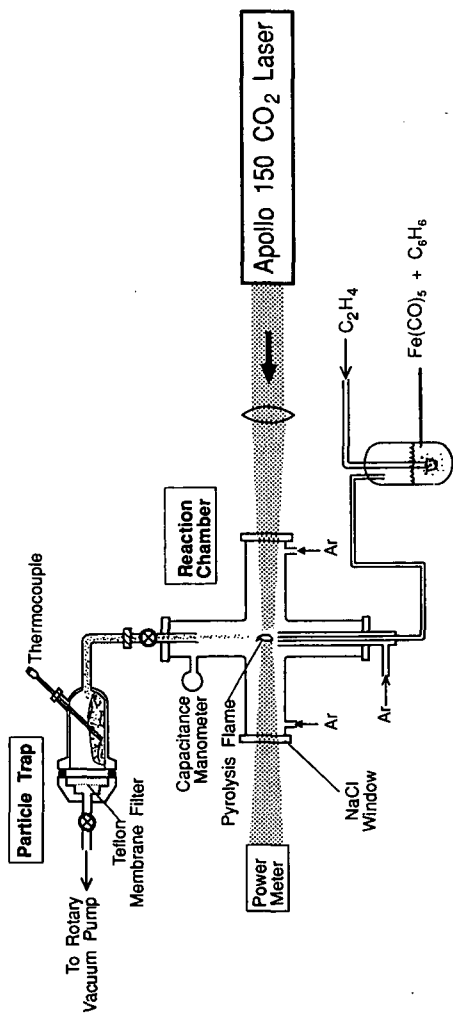
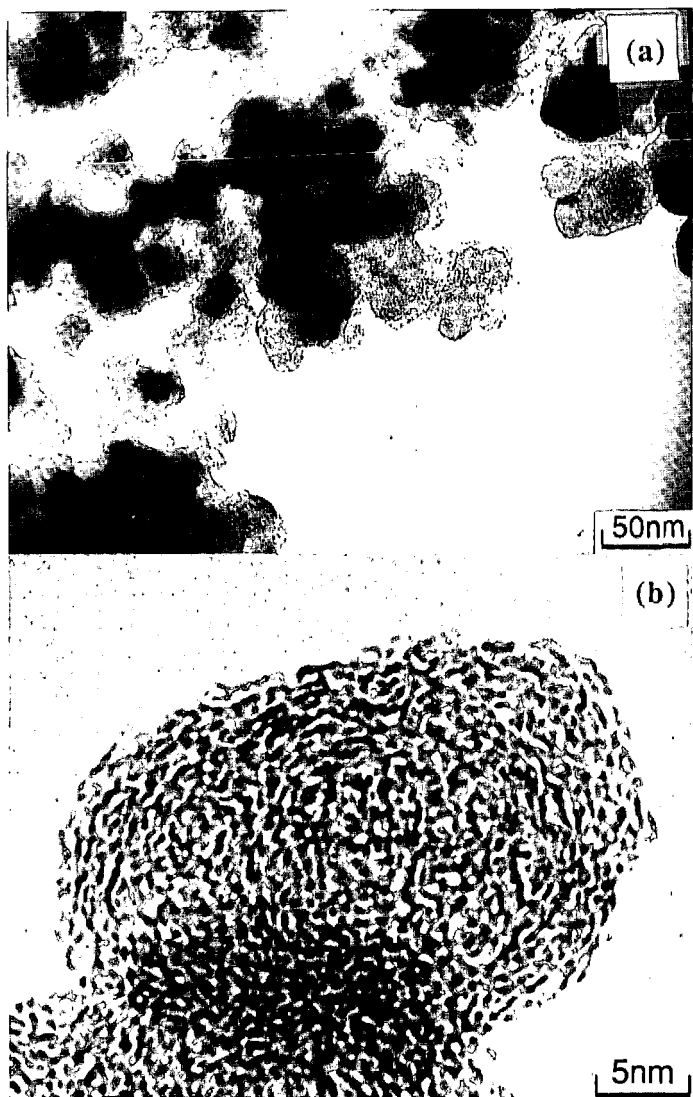
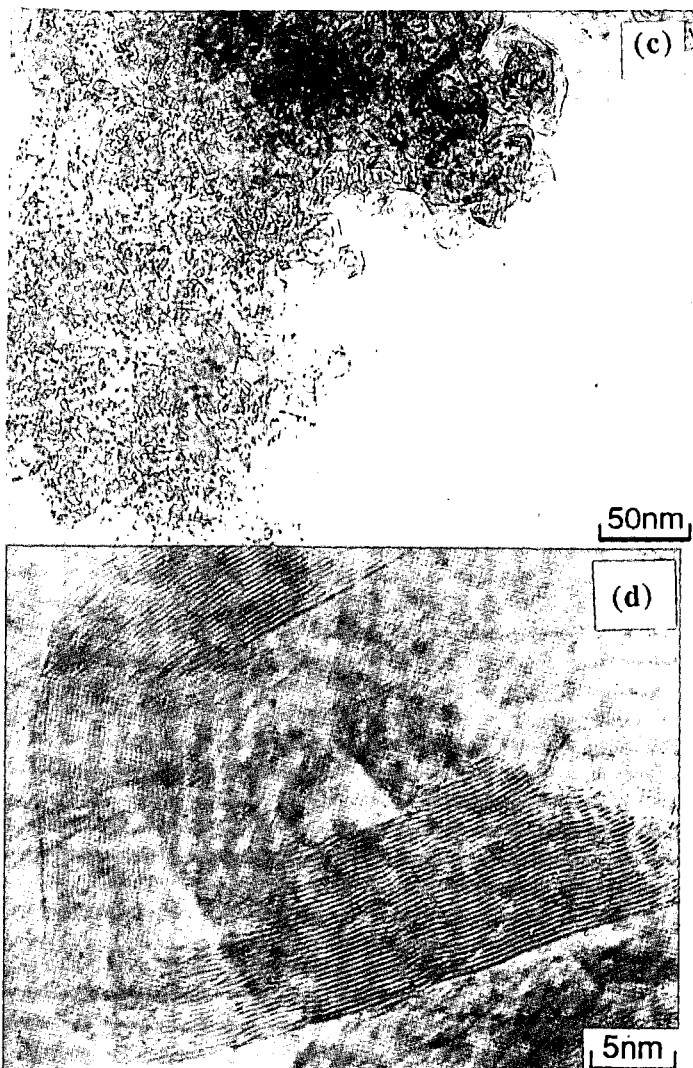


Fig. 1 Laser pyrolysis system for the production of carbon blacks.



**Fig. 2a,b** TEM data for “as synthesized” carbon blacks produced by laser pyrolysis.



**Fig. 2c,d** TEM data for heat treated (2800 °C in Ar) carbon blacks produced by laser pyrolysis.

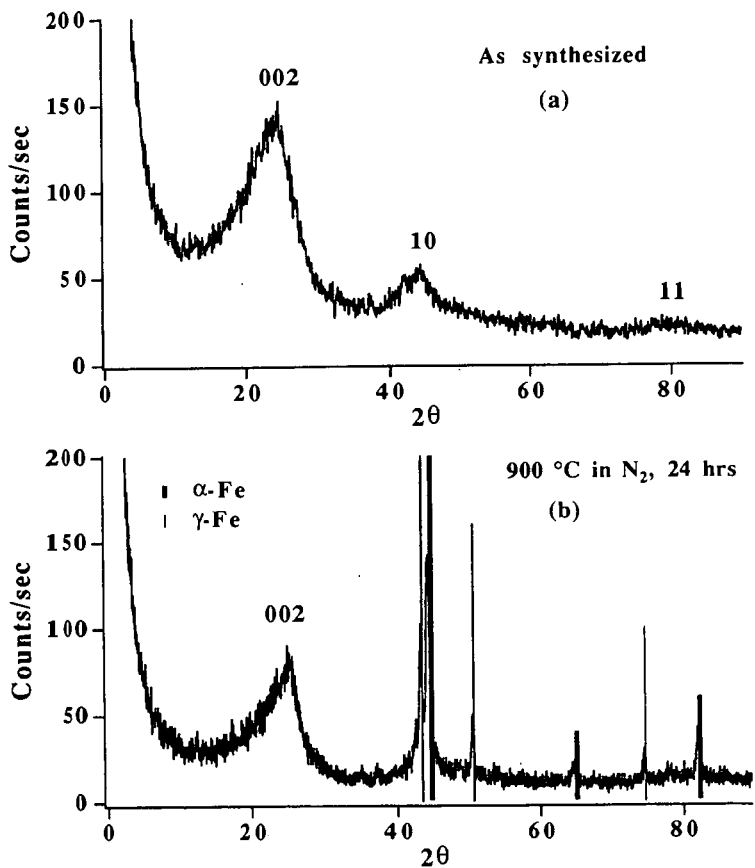


Fig. 3 XRD(Cu  $K\alpha$ ,  $\lambda=1.5418 \text{ \AA}$ ) data for "as synthesized" (3a) and heat treated (900 °C in N<sub>2</sub>) (3b) carbon black samples produced by laser pyrolysis. Vertical lines are obtained from standard powder diffraction data file.

## A GC/MS ANALYSIS AND CARBONIZATION OF DECANT OILS

S. Eser and Y. Liu

Fuel Science Program, The Pennsylvania State University  
209 Academic Projects Building, University Park, PA 16802

### ABSTRACT

Six fluid catalytic cracker decant oils (FCC-DO) samples were characterized by gas chromatography/mass spectroscopy (GC/MS) and carbonized to study the relationships between the chemical constitution and the optical texture of derived needle cokes. Ion chromatograms for each sample were studied, and more than 50 molecular and fragment ions were selected for a semi-quantitative analysis. Although the GC/MS technique and the selected ion integration method used have certain limitations, some correlation was observed between the chemical constitution of the decant oils and the quality of the resulting needle cokes.

### INTRODUCTION

Fluid catalytic cracker decant oil is used as feedstock to produce premium needle cokes. However, FCC decant oils may have significantly different chemical composition and carbonization behavior(1). Gas chromatography(GC) and size exclusion chromatography(SEC) were used to characterize carbonization feedstocks(2, 3). Recently, two-dimensional high performance liquid chromatography(HPLC) and heated probe MS analysis were developed and applied to FCC decant oil characterization(4). The reported results indicate that compounds up to seven or eight ring aromatics are found in decant oils, but in general, three and four ring aromatics and long chain normal alkanes were found to be the dominant components in decant oils(4). These results suggest that the distribution of major components in decant oil can be studied by GC/MS methods. In this study, six samples from four decant oil sources were analyzed by GC/MS using the selected ion integration method. The Carbonizations of decant oils were also carried out to study the relationships between chemical constitution of decant oils and resulting semi-cokes.

### EXPERIMENTAL

GC/MS analysis was carried out on FCC decant oil samples designated FDO #1 to FDO #6. FDO #1 and FDO #2 were received from the same source but at different time, as were samples FDO #5 and #6. An HP 5890 Gas

Chromatography interfaced to an HP 5971A Mass Selective Detector was employed. The samples were dissolved in chloroform and injected, using the splitless mode, into a J&W DB-17 GC column. The GC column temperature was controlled from 40 °C to 280 °C at heating rate of 4 °C/min.

Decant oils were carbonized in tubing reactors at 500 °C for 3 hours under a nitrogen atmosphere. Semi-cokes obtained after carbonization were embedded in epoxy resin and polished using conventional techniques. A polarized-light microscope (nikon-microphot-FXA II) was used to examine the optical textures of resultant semi-cokes.

## RESULTS AND DISCUSSION

A GC/MS total ion chromatogram (TIC) for samples FDO #1 to FDO #6 are shown in Figure 1. Most abundant ion peaks in FDO #1 and #2 are normal alkanes. Aromatic compounds become gradually important in going from FDO #1 to FDO #6. The dominant compounds in samples FDO #5 and #6 are pyrene and its methyl substituted analogs. For all the samples, constituent compounds consist of two to four ring aromatics with different degrees of ring substitution. The GC/MS TIC shows a hump of unresolved peaks around 45 to 65 minutes of retention time for each sample. A method of using selected ion chromatograms was employed to resolve the overlapping peaks.

Selected Ion Chromatograms(SIC) of mass 57, a stable aliphatic fragment, for samples FDO #1 to FDO # 6 are shown in Figure 2. All the samples show a long chain alkane distribution from C16 to C32 except sample FDO #4, which shows a significant shift towards the lower molecular weight alkanes (C12-C26). Sample FDO #3 shows a bimodal distribution of normal alkanes.

All the major aromatic peaks have been identified by mass spectroscopy. They are categorized into four series of compounds: naphthalenes, three ring aromatics (phenanthrene and anthracene), peri- and cata- four condensed ring aromatic compounds. Chromatograms of selected ions for these compounds, including alkyl substituted analogs and alkanes for FDO #3, are plotted in Figure 3. The labels "A, B, C, D" following ion mass numbers represent different isomers of the same compound. Table 1 gives the compound identification of the mass numbers used in Figure 3. Integrated intensities for ions of mass 55, 57, 69, 71, 83, 85, 97, 99 and 113 were obtained from one peak, the maximum alkane peak in each MS chromatogram.

The areas for isomers from each ion were added and the sum was divided by the area of the pyrene peak for normalization. The distribution of these summed ratios is presented in Figure 4. Columns marked alkane

present the sum of peak area ratios for 55, 57, 69, 71, 83, 85, 97, 99 and 113. Samples FDO #1 and FDO #2 show similar component distributions. The alkane contents in these two samples are higher than the other samples. Furthermore, the three ring aromatics are the most abundant components in samples FDO #1 and #2. Samples FDO #1 and #2 produced inferior optical textures upon carbonization. In contrast, samples FDO #5 and #6 produced premium needle cokes. These two samples contain less alkanes than the other samples. The dominant components in FDO #5 and #6 are pyrene and alkyl pyrenes. Sample FDO #3 contains more alkanes than FDO #4, but the former sample produced significantly better semi-coke than the latter. This implies that alkane composition may not be the only factor to affect needle coke quality. Both aliphatic and aromatic component distributions for sample FDO #4 are shifted toward lower molecular weight compound direction. This reveals why FDO #4 produced poor semi-coke.

#### REFERENCE

1. Mochida, I. ; Korai, Y.; Nesumi, Y. and Todo, Y. *Carbon* **1989**, 3, 357
2. Lewis, L. C. *Carbon* **1982**, 20(6), 519
3. Greinke, R. A. and Singer, L. S. *Carbon* **1988**, 26(5), 665
4. Liu, Y.; Eser, S. and Hatcher, P. G. *Am. Chem. Soc., Div. Fuel Chem., Preprints* **1992**,37(3), 1227

Table 1. List of selected ions

Mass	compound's name
128	Naphthalene
142	Naphthalene -methyl
156	Naphthalene -ethyl or dimethyl
170	Naphthalene -C3
178	Phenanthrene
192	Phenanthrene methyl
206	Phenanthrene ethyl or dimethyl
220	Phenanthrene - C3
202	Pyrene
216	Pyrene -methyl
230	Pyrene -ethyl or dimethyl
244	Pyrene -C3
228	chrysene
242	chrysene -methyl
256	chrysene -ethyl or dimethyl
270	chrysene -C3
55	n-C4 alkene
57	n-C4 alkane
69	n-C5 alkene
71	n-C5 alkane
83	n-C6 alkene
85	n-C6 alkane
97	n-C7 alkene
99	n-C7 alkane
113	n-C8 alkane

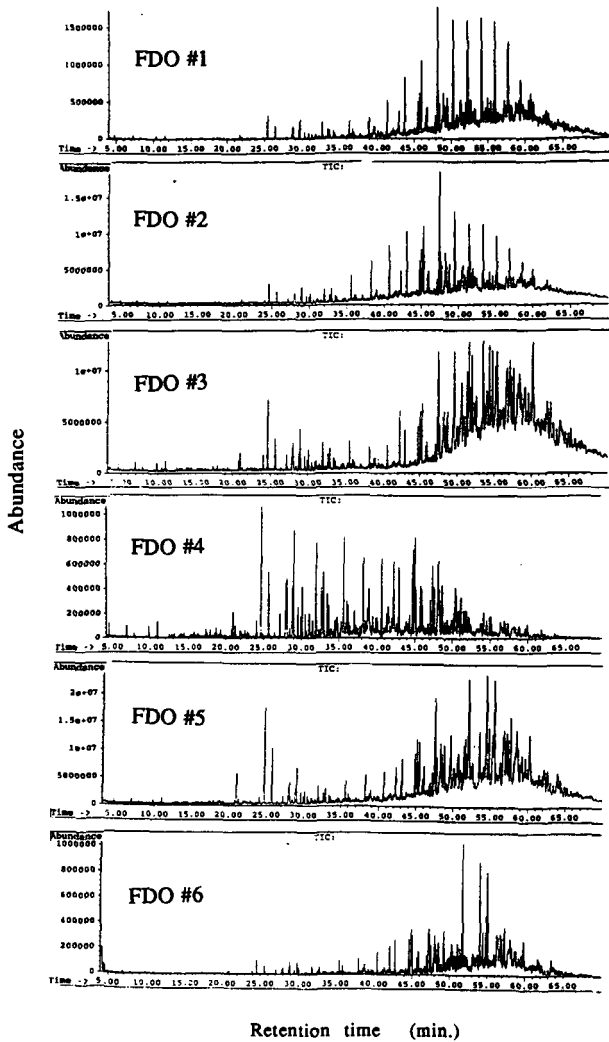


Figure 1. Total ion chromatograms for samples FDO #1 - #6

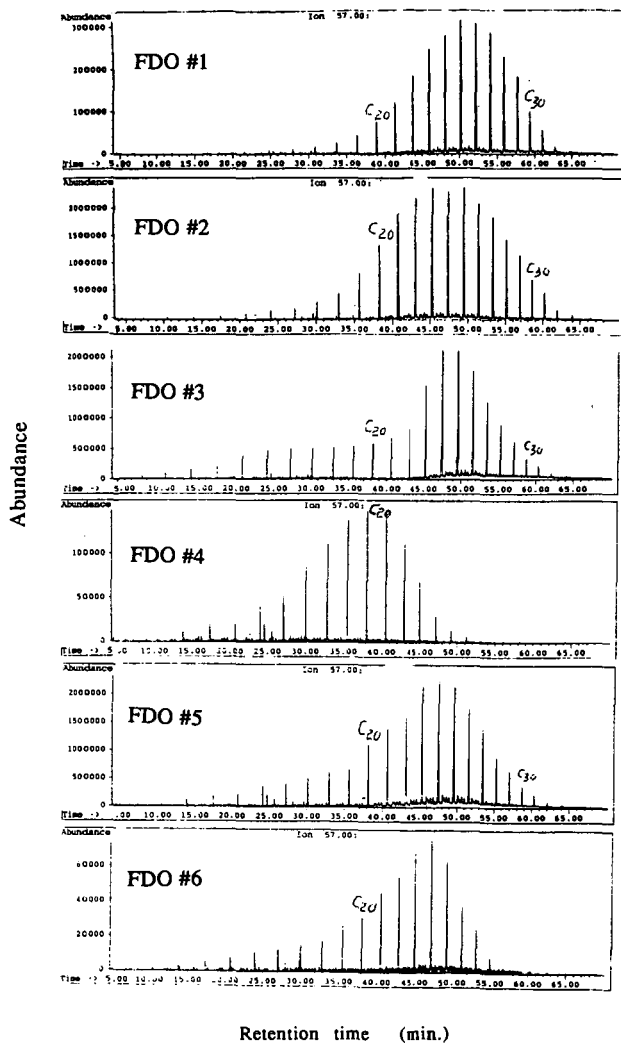
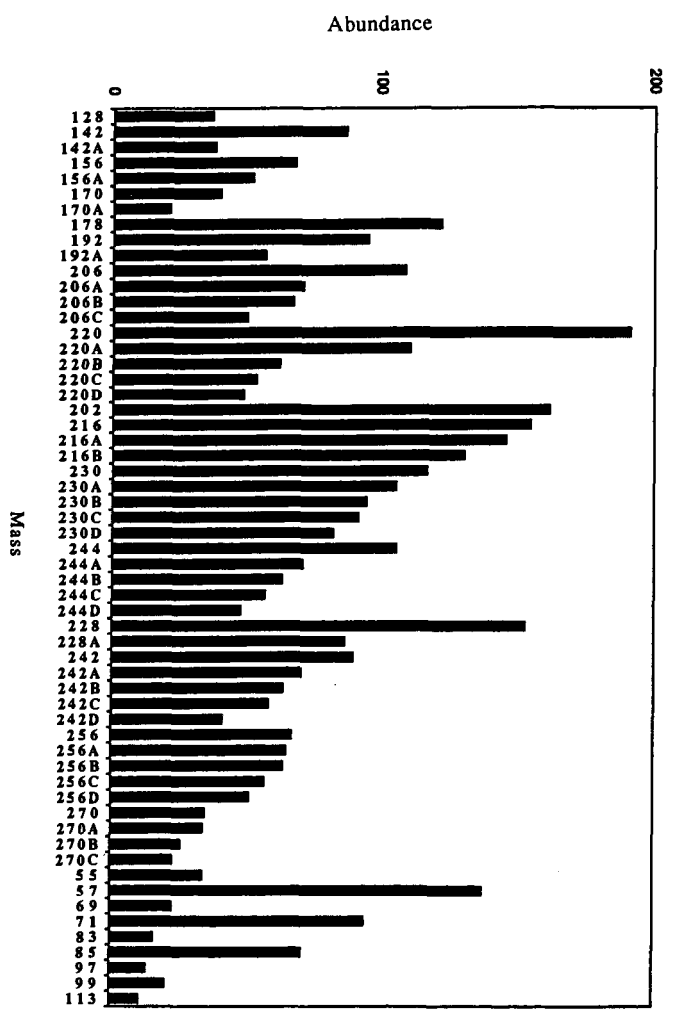


Figure 2. Selected ion (mass 57) chromatograms for FDO #1 - #6

Figure 3. A distribution of selected ions for decant oil FDO #3



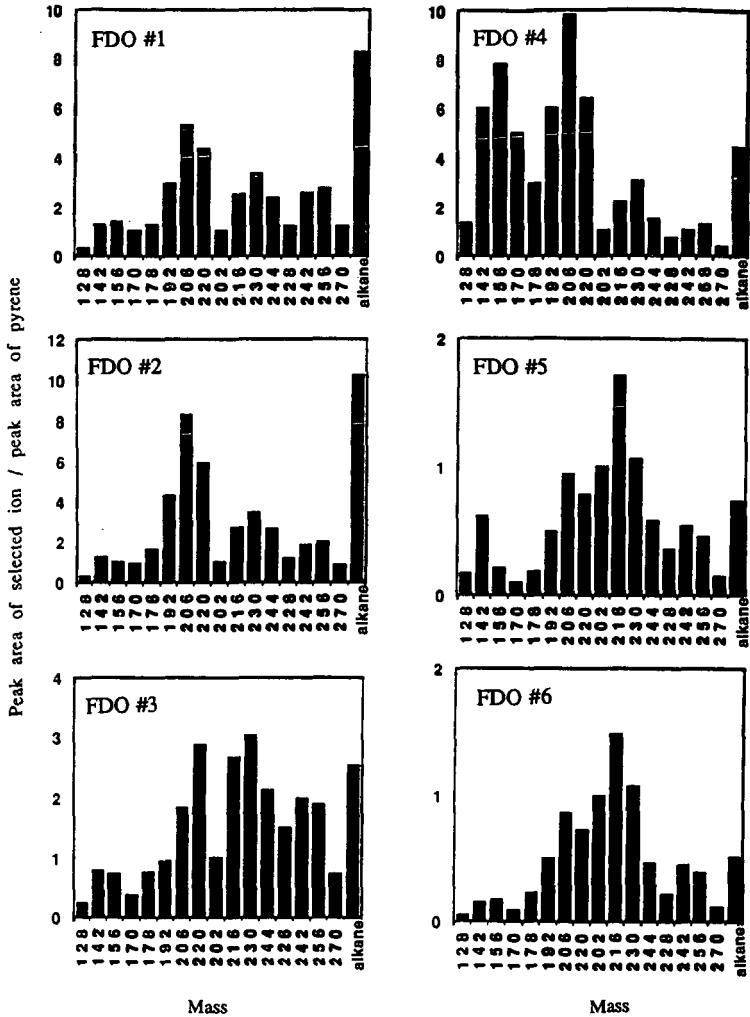


Figure 4. A distribution of selected ions for decant oil FDO #1 -#6

**CHARACTERIZATION OF THE PRODUCTS OF MILD GASIFICATION  
AT THE UNIVERSITY OF NORTH DAKOTA ENERGY AND ENVIRONMENTAL  
RESEARCH CENTER**

Brian D. Runge, Robert O. Ness, Laura Sharp  
Energy and Environmental Research Center  
University of North Dakota  
Box 8213, University Station  
Grand Forks, ND 58202

**Keywords:** Mild Gasification, Value-Added Products, Coal Utilization

**ABSTRACT**

The primary objective of the Energy and Environmental Research Center (EERC) Mild Gasification project has been to demonstrate a process that will produce several value-added products from a high-sulfur midwestern bituminous or a low-sulfur western subbituminous coal. Indiana No. 3 and Wyodak were the coals used for the majority of testing. The products of the process are a low-Btu gas, a hydrocarbon condensate, and a low-volatile char.

The testing was carried out on 4- and 100-lb/hr units. Initial yield data were generated using the 4-lb/hr continuous fluid-bed reactor (CFBR). The preliminary data were then used to plan production runs on the 100-lb/hr process research unit (PRU). An extensive survey was conducted to determine possible markets for the products. The survey indicated that the best slate of products would consist of a metallurgical form coke product from the solids, a feedstock for specialty chemicals from the liquids, and the gas being burned in the plant for utility heat or in a small electric cogeneration unit. The program was then tailored in an attempt to optimize the raw products to meet the industry standards for the desired end products. In the area of form coke, the EERC investigated organic and inorganic binders in both pelletizing and briquetting schemes. The heavy pitch fraction of the liquid products can be utilized as an organic binder in the briquetting process. The lighter liquids have been analyzed to determine their potential as a source of cresylic acid as well as for use as a liquid motor fuel.

**INTRODUCTION**

Coal is the largest indigenous energy resource in the United States. As the price of oil, both foreign and domestic, increases, it will become necessary to tap America's vast coal reserves to augment and in some cases to replace the use of petroleum. The replacement of oil with coal in production of electric power is relatively simple, and the EERC also proposes the use of coal in the chemical market.

The mild gasification process is similar in concept to an oil refinery in which a varied slate of products can be produced from a raw feedstock. The capability to alter product distributions, either by changing feedstocks or process conditions, would permit timely response to the ever-changing market. The current mild gas process consists of a rapid devolatilization of raw coal under mild conditions of temperature and pressure, resulting in a low-Btu gas, a hydrocarbon condensate, and a reactive, low-volatile char.

**RESULTS**

The major findings of the work at the EERC in mild gasification are summarized based on data from the tests on Indiana No. 3, Wyodak, and Cannelton coals in the thermogravimetric analyzer (TGA), the CFBR, and the PRU. All yields reported are as percentages of moisture- and ash-free coal.

## The Effect of Process Conditions on Char Yield and Char Quality for Indiana No. 3, Wyodak, and Cannelton Coals

### PRU Test Results

Operability of the PRU carbonizer was satisfactory for both the Indiana No. 3 and Wyodak coals. Table 1 shows the char yields and char quality from tests on the PRU and CFBR. The Indiana char values are for cleaned and uncleaned char. The lower yields for the cleaned char are due to the amount of char that is rejected in each gravity/magnetic separation that occurs between processing steps. No internal oxidation was assumed, which raised the carbonizer yield by 16%. Internal oxidation was only used to maintain reactor temperature due to heat loss.

The Wyodak char was the only char that met metallurgical coke specifications. The volatile content was higher than typical coke; however, testing indicated that briquettes produced from this char had acceptable strength properties. The Cannelton char data are reported without physical cleaning. If the relative reduction of ash in the Indiana No. 3 char can be used as a comparison, the Cannelton char could be reduced to 12%-13% ash, which would be slightly higher than the specifications. The volatile content is quite low, which should produce a high-strength coke substitute. The Indiana char did not meet the ash or sulfur content desired.

Char yields in the PRU with internal oxidation for the Indiana tests varied from 44.9% to 59.3% over a temperature range of 1020° to 1200°F (550° to 650°C) with limited agglomeration that presented no operational difficulties. The major variation was due to oxidation in the reactor for some test points in order to meet the desired run temperature. Only one mass balance was completed for the Wyodak coal, which had a yield of 49% at 1100°F (600°C).

### CFBR Test Results

Operability of the CFBR was satisfactory on noncaking Wyodak subbituminous coal. Satisfactory operation on mildly caking Indiana No. 3 and Cannelton bituminous coal was accomplished only by temperature staging, using char produced at lower-temperature runs as feed for a subsequent run at a higher temperature. Temperature stages used were 660°, 750°, 840°, 930°, and 1470°F (350°, 400°, 450°, 500°, and 800°C). Other methods that were tried for controlling agglomeration were of very limited success, including preoxidation of the coal feed, internal oxidation, and use of a limestone bed.

Char yields were determined in the CFBR between 930° and 1110°F (500° and 600°C) for Wyodak coal, at staged temperatures between 660° and 1470°F (350° and 800°C) for Indiana No. 3 coal, and at staged temperatures between 660° and 1290°F (350° and 700°C) for the Cannelton coal. The char yields decreased with increasing temperature and were significantly higher for the Indiana No. 3 coal, which yielded about 74 wt% char at 930°F (500°C) and 61 wt% at 1470°F (800°C). Corresponding yields for Wyodak were about 60 wt% at 930°F (500°C) and 50 wt% at 1110°F (600°C). Yields for the Cannelton coal were 82 and 74 wt% at 930° and 1290°F (500° and 700°C), respectively.

A calcining temperature of 1470°F (800°C) was needed to reduce the volatile content of the Indiana No. 3 char below 10%, as required for use in form coke. At this temperature, a typical analysis for Indiana No. 3 char was 8.5% volatile matter, 74% fixed carbon, 19% ash, and 3.4% sulfur without upgrading.

## **The Effect of Process Conditions on Condensable and Gas Yields**

### **PRU Test Results**

A wide variety of yields and boiling point distributions were observed for the three coals, as shown in Table 2. This table has data from the PRU and the CFBR. The Wyodak condensables approximated a liquid that was lighter than a decant oil (#6 diesel). The Indiana No. 3 liquids were the lightest and produced a 17.8% yield. Gas yields are shown in Table 3. The Indiana No. 3 yields are adjusted for no internal oxidation, which resulted in a reduction of CO<sub>2</sub>.

Initially, operation difficulties were encountered with the tar scrubber. The problems were eliminated by lowering the outlet temperature of the tar scrubber and redesigning the scrubber cyclones to eliminate mist entrainment. This increased the amount of liquid condensed in the scrubber, decreasing the coal fines/liquid ratio. The lower outlet temperature increased the light oil content of the recycle loop. This light oil then acted as a solvent for the heavy tars.

The sieve tower and water scrubber performed very well over a wide range of gas velocities and heat loads. During the course of operation, the outlet temperature of the sieve tower was reduced to below the dew point of water, in response to the reduction in outlet temperature of the tar scrubber. This reduced the heat duty on the water scrubber that served as a backup unit to remove entrained organics from the sieve tower.

### **CFBR Test Results**

Total gas yield for the Wyodak coal ranged from 31% to 51% between 930° and 1110°F (500° and 600°C), generally increasing with temperature. The total yield of gas from Indiana No. 3 coal ranged from a low of 2% to 5% at 660°F (350°C) to about 20% at 1470°F (800°C). Yields of all major gas components generally increased along with temperature. The measured gas compositions varied widely, but typical ranges were 50% to 70% for CO<sub>2</sub>, 8% to 14% for CH<sub>4</sub>, 3% to 12% for CO, and up to 3% for H<sub>2</sub>.

Yields of condensable organic liquids were higher for Indiana No. 3 bituminous coal than for Wyodak subbituminous. The cumulative yields obtained by staged heating of Indiana No. 3 coal increased along with temperature from less than 1% at 660°F (350°C) to about 18% at 930°F (500°C) and remained at 18% at the calcining temperature of 1470°F (800°C), owing to essentially zero liquid yield upon further heating of product char prepared at 930° to 1470°F (500° to 800°C). The maximum yield was less than that predicted by the Fischer Assay correlation, possibly due to the short residence time of the fine coal/char feed fraction in the fast fluidized-bed reactor.

The liquid yield for Wyodak coal was highest (10.7%) at the lowest test temperature of 930°F (500°C), and decreased by varying amounts to levels between 0.2% and 9.7%, depending on the gas atmosphere in the carbonizer.

The gas yield for the Cannelton coal was considerably lower than for the other two coals. Yields varied from 5% to 8% at temperatures from 930° to 1290°F (500° to 700°C). Condensable yields ranged from 14% to 19% over the same temperature range, with a large quantity in the 430° to 700°F (220° to 370°C) boiling point range. The most important feature of the Cannelton liquids was the quality. It resembled a #3 diesel fuel.

### **The Effect of Gas Atmosphere Including Steam on Liquid Yield and Quality (CFBR Test Results)**

The use of steam increased the liquid yield from Wyodak coal in three different gas atmospheres, including 1) CO<sub>2</sub>; 2) N<sub>2</sub>/CO<sub>2</sub>, representing flue gas; and 3) N<sub>2</sub>/CO<sub>2</sub>/2% O<sub>2</sub>, representing flue gas with

excess air. The effect of steam was noted primarily at the highest test temperature of 1110°F (600°C), where in all cases an increase in steam partial pressure caused an increase in liquid yield, which, in the case of the  $N_2/CO_2$  gas atmosphere, amounted to an increase from 0.2% liquid at 21% steam to 9.7% at 88% steam. The presence of 2%  $O_2$ , surprisingly, did not reduce the liquid yield, which was higher with 2%  $O_2$  than for  $N_2/CO_2$  alone at a low-steam partial pressure and which was about the same at higher levels of steam. At the lower temperatures of 1020° and 930°F (550° and 500°C), the Wyodak liquid yield varied with steam partial pressure in a manner that did not define a systematic trend.

For Indiana No. 3 coal, liquid yield increased consistently, but only slightly, along with an increase in steam at lower staging temperatures between 660° and 750°F (350° and 400°C). At higher temperatures, no consistent trend was observed.

The boiling point profiles and compound distributions for the two test coals differed, as shown in Table 4. The 3% to 4% low boiling aromatic fraction (BTX) is believed to be lower than the amount actually produced because of losses in the condensation train. Wyodak coal when carbonized without steam produced the highest yield of phenolics, boiling between 330° and 430°F (170° and 220°C). The 430° to 700°F (220° to 370°C) fraction was higher for Indiana No. 3 coal, but the even higher boiling pitch fraction was nearly missing for this coal as tested.

The most prominent effect of steam was to promote higher liquid yields from Wyodak coal at the higher carbonization temperature of 1110°F (600°C). At this condition, the steam is believed to have prevented the retrograde condensation and polymerization of organic compounds on the highly reactive surface of the Wyodak char. Another possible scenario is that the steam provides a better mechanism for removing the tar from the char pore structures. At any given temperature, the condensable yield with steam produced an amount of liquids equivalent to that produced under a higher operating temperature without steam.

#### **The Effect of Process Conditions on Sulfur Removal**

Sulfur reduction played a major role in the development of the process, as the main feed coal had a sulfur content over 4.2%. Since the program was to provide engineering data for commercialization, only proven, low-cost sulfur-reduction techniques were reviewed and incorporated into the process.

A series of tests were conducted to establish the database using a TGA and the CFBR in conjunction with analytical techniques that include scattered electron microscopy (SEM) with elemental mapping. A summary of the findings on in-process sulfur removal includes the following points:

- Pyritic sulfur was effectively reduced to low levels, but organic sulfur, as defined by ASTM analytical methods, was not appreciably reduced.
- Residence time had an important influence on the amount of pyritic and total sulfur removed. The effect extended beyond the 20- to 30-minute residence time at staging temperatures in the TGA and CFBR, since the greatest reduction in total sulfur content (from 3.9% to 1.2%) was observed after 6 hours of residence time in the 30-lb/hr fluidized-bed reactor.
- Gas atmosphere had a minor effect on sulfur removal. Larger reductions in total sulfur content in TGA tests were noted in either reducing ( $CO$  or  $H_2/CO$ ) or oxidizing atmospheres than in  $N_2$ . The use of steam in the 4-lb/hr CFBR did not increase the extent of sulfur removal.

- The chemical forms of sulfur in char were found to be more complex than the pyritic, sulfitic, and organic forms defined by the ASTM procedure. Analysis of char surfaces using scanning electron microscopy/energy dispersive spectroscopy (SEM/EDS) and electron spectroscopy for chemical analysis (ESCA) indicated that important changes in the physical and chemical form of sulfur occurred at 720° to 840°F (380° to 450°C) coincident with the onset of coal agglomeration and with the loss of sulfur from pyrite (FeS<sub>2</sub> to FeS). The principal change observed was that discrete crystals containing sulfur (possibly pyrite) present at 660°F (350°C) had disappeared at 840°F (450°C) and were replaced by a low concentration of sulfur that was detected over the entire char surface. SEM mappings of elements indicated some coincidence in the location of sulfur with Fe and Ca.
- After heating to calcining temperatures, most of the sulfur remaining in the coal is in the ASTM organic form. No combination of time, temperature, and gas atmosphere investigated in this study was successful in systematically removing this stable form of "organic sulfur."

#### **Results of Char Upgrading for the Production of Metallurgical Coke Substitutes Using Inorganic Binders (PTC Process)**

Table 5 includes a compilation of the compressive strengths, impact numbers, and tumble tests for the green pellets, dried pellets, and hardened pellets for the char with/without limestone. The individual tests for inorganic and organic binders use slightly different methods, so only general comparisons can be made between the two binders.

The initial Wyodak char submitted to Pellet Technology Corporation (PTC) for testing contained an uncharacteristically high ash content of 27%, owing to contamination from the limestone bed in the 30-lb/hr fluidized-bed reactor used to produce this bulk sample.

- CaO-SiO<sub>2</sub>-bonded carbon pellets and carbon-iron ore pellets of 1-inch diameter were successfully produced by induration in saturated steam at 420°F (215°C) and 300 psig.
- The finished pellets exhibited satisfactory strength, density, and abrasion resistance with 10% CaO-SiO<sub>2</sub> binder, but not with 5% binder. Since the addition of inorganic binder increases the amount of slag in the iron smelting process, a smaller amount of binder would be a significant benefit.
- The char-iron ore pellets were reduced to iron metal at very high rates upon heating to 2700°F (1480°C). The 5 minutes required for reduction was estimated to be fivefold less than it would have been using coke-iron ore pellets, owing to the high reactivity of the Wyodak char.

The inorganic tests yielded marginally acceptable compressive strength pellets for the Indiana No. 3 and Wyodak chars. The char-iron ore agglomerates were superior in all categories. The sulfur and volatile contents of the agglomerates are considerably lower since they are made of 25% char and 75% iron ore.

#### **Results of Char Upgrading for the Production of Metallurgical Coke Substitutes Using Organic Binders**

The Wyodak and Indiana chars were briquetted using a variety of organic binder types and binder levels that ranged from molasses and starch acrylic copolymer emulsions to coal-derived liquids. The briquettes were then subjected to compressive strength, tumble, and impact tests for the purpose of comparison with PTC pellets. The following is a summary of the organic binder briquette tests:

- Indiana and Wyodak chars when mixed with the asphalt emulsions, FMC formcoke® pitch, P028 scrubber tar, and P027 scrubber tar distillation resid as binders yielded durable oven-cured tablets with high compressive strengths.
- When the briquettes of Indiana char together with 15 wt% P027 scrubber tar distillation resid and the briquettes of Wyodak char with 20 wt% P028 scrubber tar were coked, their strength approached that of FMC formcoke®.
- Wyodak or Indiana char briquettes containing 15 wt% or less P028 scrubber tar or 15 wt% asphalt emulsion did not meet the strength criteria.
- Coked Indiana and Wyodak char briquettes were resistant to moisture absorption under simulated conditions of water soaking and rain showers.
- Wyodak char briquettes, with strength and durability similar or superior to that of a commercial barbecue briquette, can be prepared using starch binders at concentrations of ~4 wt%. Exceedingly strong briquettes with almost complete shatter and abrasion resistance can be prepared with 7 wt% starch.

Table 5 includes a compilation of the compressive strengths, impact numbers, and tumble tests for the dried pellets and hardened pellets for the two chars. The two examples shown in the table are those with the coal-derived liquid. The Wyodak pellet had a high sulfur content due to the use of Indiana tar as the binder, and the char produced was a combination of Wyodak and Indiana No. 3 char.

#### **Results of Char Upgrading for the Production of Activated Carbon**

The production of activated carbon for use in the adsorption of SO<sub>2</sub> was investigated by producing calcined char with a small amount of steam present in the reactor. The resulting char was pelletized using the PTC process to provide a uniform particle of sufficient size and strength to be used in a filter device.

Sulfur capture was determined by using a TGA with an argon/sulfur dioxide sweep gas. The activated carbon produced at 1380°F (750°C) with 26% of the fluidization gas being steam had the highest SO<sub>2</sub> adsorption. The char increased in weight by 8.1%. Pelletizing the char had no effect on the adsorption capabilities of the char and produced a product that had much better material-handling capabilities. Higher steam partial pressures should be investigated as the experimental matrix did not find the upper limit of steam partial pressure in relation to increased SO<sub>2</sub> adsorption.

#### **Results of Condensable Upgrading for the Production of Cresylic Acid**

The Indiana No. 3 liquids yielded cresylic acids in quantities less than 5% of the original sample. It would not be economical to recover such a small quantity of cresylic acid from the liquid stream. However, the Wyodak condensables that were provided to Merichem from the Western Research Institute (WRI) mild gasification project contained 40% usable cresylic acids. This amount merits further consideration into the economic merits.

#### **Results of Condensable Upgrading for the Production of Diesel Fuel Additives**

The results from the diesel fuel testing being conducted by Oak Ridge National Laboratories under a separate DOE contract were not available by the publication deadline.

TABLE 1. Char Yields and Quality

Coal Specifications	Coal			
	Wyodak <sup>a</sup>	Indiana <sup>b</sup>	Indiana <sup>c</sup>	Cannelton
930°F	60.0	74.0		81.7
1110°F	49.0	68.0	54.4	
1290°F		55.1	30.1	74.3
Proximate Analysis, wt%				
Temperature, °F	1110	1290	1290	1290
Fixed Carbon	74.6	65.3	59.6	73.1
Volatiles	< 10	15.0	10.3	6.7
Moisture		1.5	2.0	0.5
Ash	< 10	8.9	22.5	16.1
Sulfur	< 1	0.5	3.5	2.9

<sup>a</sup> Uncleaned.

<sup>b</sup> No internal oxidation.

<sup>c</sup> Cleaned (low yields due to coal reject in cleaning steps).

TABLE 2. Condensable Yields and Quality

	#2 Diesel Decant Oil		Wyodak		Indiana		Cannelton		
	%	%	Yield	%	Yield	%	Yield	%	
ibp - 330°F	10		0.3	3	0.7	4	0.1	1	Gasoline Octane Enhancers, Benzene Cresylic Acids, Phenols Diesel Fuel Blends Briquetting Binders, Anode Carbon
330° - 430°F	86		3.2	34	6.2	35	2.7	14	
430° - 700°F	4	44	3.9	41	10.7	60	14.1	74	
700° - 1020°F		56	2.1	22	0.2	1	2.1	11	
	100	100	9.5	100	17.8	100	19.0	100	

TABLE 3. Gas Yields

	Wyodak	Indiana <sup>a</sup>	Cannelton
930°F	31.0	10.0	5.0
1110°F	42.0	19.0	
1290°F		22.0	8.0

<sup>a</sup> No internal oxidation.

TABLE 4. Comparison of Wyodak and Indiana No. 3 Condensable Boiling Point Fractions

Boiling Point Range and Major Compound Type	Percent of Liquid Produced		
	Wyodak 1110°F 0% Steam	Wyodak 1110°F 99% Steam	Indiana Staged to 1470°F 30% Steam
ibp to 330°F, BTX	4.0	3.4	3.6
330° to 430°F, phenolics	44.0	34.1	35.4
430° to 700°F, multiring aromatics and alkylated phenolics	34.7	40.6	59.6
above 770°F, crude pitch	17.4	21.9	1.4

TABLE 5. Summary of Inorganic and Organic Pelletizing Tests<sup>a</sup>

	Indiana No. 3		Indiana No. 3 <sup>b</sup>		Wyodak		Wyodak <sup>b</sup>		Indiana No. 3		Wyodak	
	PTC Process Inorganic Binder											
Inorganic Content	24.4	76.2	28.0	77.9	47.8	27.0	21.0					
Sulfur Content	3.3	0.6	0.8	0.2	0.6	2.8	3.0					
Volatile Content	10.6	2.1	10.2	2.1	7.7	<6.0	6.4					
Green Pellets												
Compressive Strength, lb	13.6	7.7	16.7	9.9	80.6							
Impact Number	>26.0	6.4	>25.0	12.3	46.6							
Dried Pellets												
Compressive Strength, lb	6.4	6.4	7.7	7.0	1.5	108.0	89.0					
Impact Number	2.0	1.0	2.0	1.6	1.6							
Hardened Pellets												
Compressive Strength, lb	20.3	146.4	46.2	104.0	340.0	163.0	64.0					
Impact Number	6.2	>25.0	16.8	>25.0	>100							
Density, g/cm <sup>3</sup>	1.3	2.5	1.0	2.4	2.1	1.1	1.0					
Tumble Test, %												
+3 mesh	68.0	98.0	92.5	97.2	98.2	89.0	87.0					
+14 mesh	2.8	0.2	0.2	0.1	0							
-14 mesh	29.2	1.8	7.4	2.7	1.8							

<sup>a</sup> Numbers reported are those for the coke produced that provided the best specifications. The PTC pellets reported here are only char.

<sup>b</sup> Iron/char agglomerate.

<sup>c</sup> Wyodak char contained 16% limestone.

<sup>d</sup> Crushed Indiana char with 16% coal-derived tar and 16% limestone.

<sup>e</sup> Crushed Wyodak char with 4.1% Sta-Lok and 4.6% Indiana coal-derived tar.

## **Ion Exchange Properties of Selected North American Low Rank Coals.**

C.J. Lafferty<sup>(1)</sup>, J.D. Robertson<sup>(1,2)</sup>, J.C. Hower<sup>(1)</sup> and T.V. Verheyen<sup>(3)</sup>.

1) Center for Applied Energy Research  
University of Kentucky  
3572 Iron Works Pike  
Lexington KY 40511.

2) Department of Chemistry  
University of Kentucky  
Lexington KY 40506.

3) Coal Corporation of Victoria.  
PMB No.1  
Morwell  
Victoria 3840  
Australia.

Keywords: Lignite, Ion Exchange, Metal Adsorption.

### **Introduction**

One of the main problems with the use of low rank coal for combustion purposes lies in its inherently high oxygen content. The high oxygen content results in increased coal reactivity and degradation during mining and storage as well as serving to decrease the overall calorific value of the coal. The high oxygen contents of selected low rank coals can, however, be of great value in certain situations, especially with respect to functional groups containing an exchangeable hydrogen ion.

The ability of low rank coals to form stable complexes with several heavy metal ions has long been recognized<sup>(1-8)</sup>. This property has been successfully utilized to estimate the concentration of acidic oxygen functional groups present in low rank coals<sup>(6)</sup> as well as serving as a convenient means of dispersing metal catalysts across a coal surface prior to liquefaction<sup>(9)</sup>. The relatively high ion exchange capacity of several low rank coals studied, coupled with the low overall cost of the bulk material, indicates great potential for the utilization of low rank coals as a means to remove a range of metals from aqueous waste streams.

## Experimental

The lignites chosen for investigation were from A. The Beulah Zap deposit, in Mercer County, North Dakota. B. The Claiborne Deposit in Carlisle County, Western Kentucky and C. The Jackson Group in Atascosa County, Eastern Texas. A sample of brown coal from the Loy Yang coal field in the Latrobe Valley, Victoria, Australia was also included for comparative purposes as its ion exchange properties have been well documented<sup>(1-3)</sup>.

The samples were obtained with a particle size of < 50 mesh and as such no further size reduction was carried out. The samples were received as mined and stored inside double plastic bags to prevent moisture loss from the samples.

Samples of each coal were also petrographically characterized using combined white light and blue light microscopic analysis. Maceral nomenclature was based on descriptions published in Ref.12.

The ion exchange properties of each coal was characterized using batch metal adsorption tests. Metal solutions were made from AR grade reagents and stored in glass volumetric flasks prior to use. No pH adjustment was made to any of the solutions as that would entail the addition of extra competing cations to the solutions and thus interfere with the ion exchange process. Batch ion exchange experiments were performed by shaking 50.0 mL of the metal solution with a pre-weighed mass (equivalent to 2.50 g dry weight) of as-received coal in 125 mL polyethylene bottles. The bottles were shaken for 12 hours on an orbital shaking platform to ensure equilibrium conditions were reached. The samples were allowed to settle for a further 12 hours before the supernatant solution was sampled for metal analysis using Inductively Coupled Plasma Spectrometry.

FTIR spectra were obtained from 0.4% loaded KBr discs using a Nicolet 20SX spectrophotometer. The discs were dried in vacuo over P<sub>2</sub>O<sub>5</sub> to minimize interference due to adsorbed H<sub>2</sub>O.

## Results and Discussion

### Petrographical Analysis

The four Tertiary lignites were analyzed petrographically according to humic maceral nomenclature outlined in Stach et al.<sup>(10)</sup> and through ICCP communications. Previous studies of the petrology of the Kentucky and Texas lignites were done by Hower et al.<sup>(11)</sup> and Mukhopadhyay<sup>(12)</sup>.

Mean reflectance was done on uniform ulminite fragments. No polarizer or stage rotation were employed in the reflectance analysis. The Paleocene Beulah-Zap, Mercer County, North Dakota, lignite has the highest reflectance, 0.33% R<sub>mean</sub>, followed by the Eocene Jackson Group lignite from Atascosa County, Texas, at 0.28% R<sub>mean</sub>. The Eocene Claiborne Formation lignite from Carlisle County, Kentucky, and the Loy Yang lignite from Victoria, Australia, have mean reflectances of about 0.20%. Lower ulminite amounts in

the latter two lignites hindered the reflectance analyses.

The lignites have distinctive maceral compositions. The North Dakota lignite has the highest percentage of relatively "intact" wood-derived macerals: textinite, ulminite, corpohuminite, fusinite, semifusinite versus humodetrinite. The high inertinite concentration of that sample sets it apart from the other samples.

The Texas lignite has over 50% ulminite in contrast to the high humodetrinite concentration in the Kentucky lignite. The Loy Yang lignite has the highest concentration of liptinite macerals with much of the group being liptodetrinite. The Loy Yang lignite appears to have a relatively high concentration of root-derived macerals, particularly suberinite-enclosed rootlets. The contrast between the raw and sized Kentucky and Texas lignites is also distinctive. In both cases much of the relative order of humic maceral percentages is preserved but there is an increase in the percentage of liptinite macerals in the sized fraction. Liptinite contributes to the strength of the particles and tends to be concentrated in the coarser particles. The fine particles would have had a higher percentage of humic macerals, particularly the easily fragmented humodetrinite which was lost in greater proportions than ulminite.

#### **Batch Metal Adsorption Tests.**

Table 2 lists the equilibrium metal concentrations and solution pH's measured after samples of the various lignites were contacted with 1000 ppm solutions of mercury, lead and cadmium at a solid : liquid ratio of 5:100 (measured on a dry coal basis). As expected, equilibrium solution pH was found to be the major factor determining the extent of metal adsorption. Coals that generated the higher solution pH's were found to exhibit the largest metal adsorption capacities. When analyzing solutions that had been treated with either the North Dakota or East Texas lignites, high levels of sodium were detected in the plasma during metal analysis indicating that a large proportion of the carboxylic groups in these coals are naturally present as sodium carboxylates, which explains the relatively high pH's generated in solution. Sodium carboxylates are known to exchange for a divalent cation more readily than protonated groups which accounts for the high level of metal adsorption measured for these lignites. The sample of West Kentucky lignite also displayed a relatively large adsorptive capacity for the metals investigated but did not contain appreciable amounts of sodium (as detected visually in the plasma), although the relatively high pH's generated in solution would indicate that the coal is naturally pre-exchanged with another readily exchangeable cation.

All of the North American lignites investigated showed relatively high adsorptive capacities for each of the metals investigated. Using multi-stage treatments of heavy metal solutions with these lignites, it should therefore be possible to meet EPA discharge limits much more cheaply than using conventional heavy metal treatment processes.

## Infra Red Spectroscopy

The FTIR spectra of the ROM (Run Of Mine) coals is presented in Figure 1. The spectra reveal that Loy Yang has the highest concentration of carbonyl/free carboxyl groups followed by Kentucky whilst the Texas and Nth Dakota coals contain relatively few. The spectrum of the Kentucky coal is dominated by strong adsorptions associated with clays/silicates. The Texas lignite, in addition, features adsorptions commonly associated with carbonates. Loy Yang in accord with its low ash yield contains very little adsorption associated with mineral matter.

Acid washing the ROM Kentucky coal converts the carboxylate salts to their corresponding protonated acids, Figure 2. The broad adsorption associated with carboxylates at  $\sim 1575\text{cm}^{-1}$  is merged with the  $\sim 1600\text{cm}^{-1}$  band in the ROM and metal exchanged spectra. Protonation shifts the carbonyl/carboxyl adsorption band back into the  $\sim 1700\text{cm}^{-1}$  region. Figure 2 reveals that the ROM and metal exchanged spectra are equivalent indicating that the ROM coal is naturally present in its fully exchanged form.

The positive bands in the difference spectrum (Loy Yang-Kentucky) in Figure 3, confirm the greater concentration of free carboxyl groups in the Victorian coal.

## Conclusions

Three North American lignites were studied in order to characterize their ion exchange properties. All three coals were shown to be capable of adsorbing significant quantities of mercury, cadmium and lead from solution. Infra Red spectroscopy confirmed that the metals were ion exchanged with carboxylic acid functional groups to form metal carboxylates on the coal surface. From these results it would appear that low rank coals show great promise as a means of cheaply removing heavy metal contaminants from aqueous streams. Further studies will concentrate on the ion exchange capacity and selectivity of these coals as well as investigating the possible uses of the ion exchanged coals.

## Acknowledgements

The authors thank Bill Schram for his assistance with the metal analyses.

## References

1. Lambert J.D., Lafferty C.J., Perry G.J. and Royston D., 1986, *Proc. Aust. Conf. Coal Sci.* 2, 1, 142.
2. Lafferty C.J. and Hobday M.D., 1990, *Fuel*, 69, 79.
3. Lafferty C.J. and Hobday M.D., 1990, *Fuel*, 69, 84.

4. Stuart A. D., 1986, Fuel, **65**, 1003.
5. Allen S.J., 1987, Fuel, **66**, 1171.
6. Schafer H.N.S., 1970, Fuel, **49**, 197.
7. Schafer H.N.S., 1970, Fuel, **49**, 271.
8. Schafer H.N.S., 1970, Fuel, **56**, 45.
9. Hatswell M.R., Jackson W.R., Larkins F.P., Marshall M., Rash D. and Egers E.R., 1980, Fuel, **59**, 442.
10. Stach, E., Mackowsky, M.-Th., Teichmüller, M., Taylor, G.H., Chandra, D., and Teichmüller, R., 1982, Coal petrology: Berlin, Gebrüder Borntraeger.
11. Hower, J.C., Rich, F.J., Williams, D.A., Bland, A.E., and Fiene, F.L., 1990, Int. Jour. Coal Geology, **16**, 239.
12. Mukhopadhyay, P. K., 1989, Organic petrography and organic geochemistry of Texas Tertiary coals in relation to depositional environment and hydrocarbon generation: Texas Bureau of Economic Geology, Report of Investigations 188.

**Table 1. Petrographic Composition of Lignite Samples.**

	Texas <sup>1</sup>	Texas <sup>2</sup>	Kentucky <sup>1</sup>	Kentucky <sup>2</sup>	N. Dakota	Loy Yang
Textinite	4.5	8.8	4.2	3.8	7.8	11.2
Ullminite	56.9	53.2	18.6	17.0	47.6	14.4
Humodet.	26.1	11.2	50.6	31.8	6.6	22.0
Gelinite			2.0	1.8	0.2	
Corpohum.	3.2	6.6	4.8	7.0	1.4	12.8
Fusinite		0.6	2.2	1.2	19.2	t
Semifusinite	0.6	0.4	1.0	0.2	10.8	
Sclerotinite	0.1	0.2	1.0	1.2		t
Inertodet.					1.2	
Exinite	3.8	4.2	4.6	7.8	2.6	3.2
Resinite	4.6	5.8	2.0	6.8	0.2	10.8
Suberinite	0.1	1.0	0.4	0.2	0.2	3.2
Liptodet.	0.1	7.8	6.4	20.4	2.2	22.4
Alginite			1.2			
R <sub>mean</sub>	0.28		0.20		0.33	0.19

<sup>1</sup> raw sample  
<sup>2</sup> sized sample

**Table 2. Ion Exchange Properties of Selected Lignites.**

<b>Coal</b>	<b>Mass (wet)</b>	<b>Mass (dry)</b>	<b>Metal</b>	<b>[Metal] (ppm)</b>	<b>pH</b>
Blank			Hg	1175	4.97
Loy Yang	6.82	2.32	(Chloride)	566	3.27
North Dakota	3.28	2.62		12	6.53
Blank			Cd	1105	7.11
Loy Yang	6.82	2.32	(Acetate)	128	4.37
North Dakota	3.15	2.52		45	6.55
Blank				1040	
West Ky.	3.49	2.51		116	4.91
East Tx.	3.35	2.48		78	5.64
Blank			Pb	1069	5.98
Loy Yang	6.70	2.28	(Acetate)	30	3.98
North Dakota	2.93	2.34		5	6.72
Blank				1005	
West Ky.	3.47	2.50		7	4.83
East Tx.	3.34	2.47		2	5.74

Coal shaken with 50.0 mL of solution for 12 hours, allowed to settle for approx. 5 hrs and the supernatant sampled for residual metal analysis.

Moistures:	Loy Yang	(Latrobe Valley, Victoria, Australia)	66%
	North Dakota	(Beulah Zap, Mercer Co. ND)	20%
	East Texas	(Jackson Fm, Atascosa Co. Tx)	26%
	West Kentucky	(Claiborne Fm., Carlisle Co., Ky)	28%

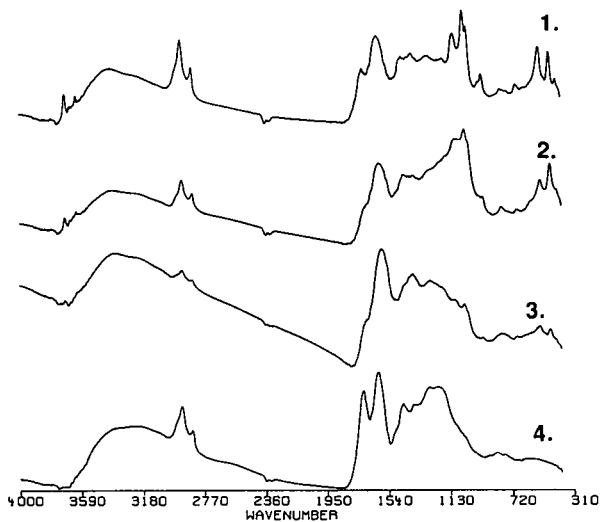


**Figure 1. Infra Red Spectra of As-Received Coals**  
 1. Kentucky 2. Texas 3. North Dakota 4. Loy Yang

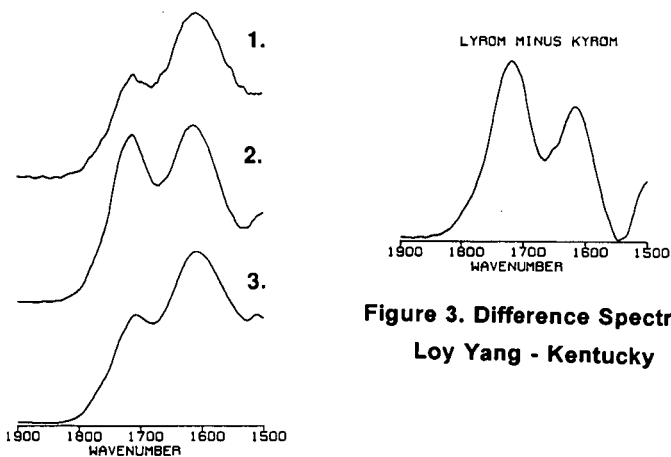


**Figure 2. Infra Red Spectra of Kentucky Lignite**  
 1. As-Received 2. Acid Extracted 3. Metal Exchanged.